

สมบัติเชิงกลและเชิงความร้อนของคอมพอสิตลิกวิคคริสตัลพอลิเมอร์และออร์แกนอเคลย์



นางสาวนุชฎี หอมเนียม

สถาบันวิทยบริการ

จุฬาลงกรณ์มหาวิทยาลัย
วิทยานิพนธ์นี้เป็นส่วนหนึ่งของการศึกษาตามหลักสูตรปริญญาวิทยาศาสตรมหาบัณฑิต
สาขาวิชาปิโตรเคมีและวิทยาศาสตร์พอลิเมอร์

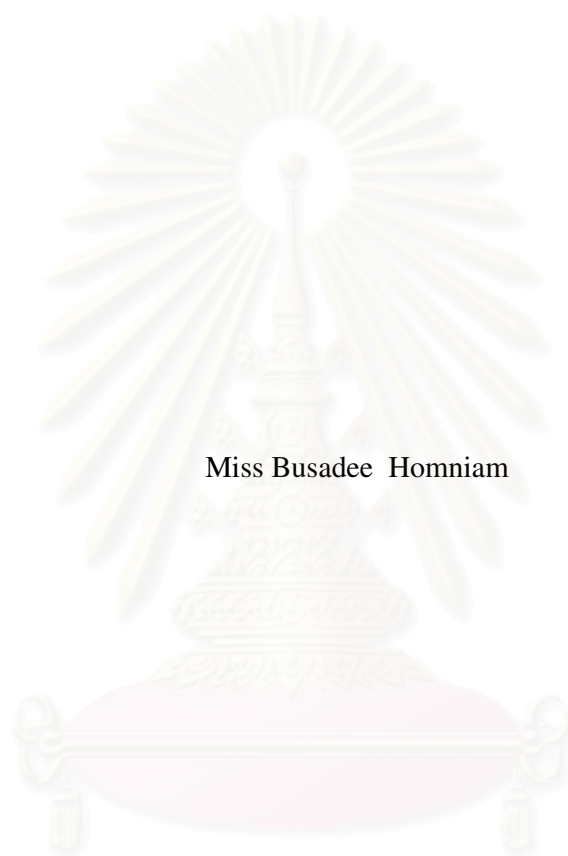
คณะวิทยาศาสตร์ จุฬาลงกรณ์มหาวิทยาลัย

ปีการศึกษา 2549

ISBN 974-14-3386-7

ลิขสิทธิ์ของจุฬาลงกรณ์มหาวิทยาลัย

MECHANICAL AND THERMAL PROPERTIES OF LIQUID CRYSTAL
POLYMER/ORGANOCLAY COMPOSITE



Miss Busadee Homniam

สถาบันวิทยบริการ
จุฬาลงกรณ์มหาวิทยาลัย
A Thesis Submitted in Partial Fulfillment of the Requirements
for the Degree of Master of Science Program in Petrochemistry and Polymer Science

Faculty of Science

Chulalongkorn University


Academic Year 2006

ISBN 974-14-3386-7

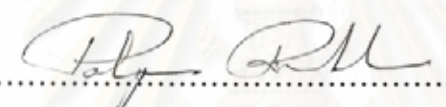
Copyright of Chulalongkorn University

Thesis Title MECHANICAL AND THERMAL PROPERTIES OF LIQUID
CRYSTAL POLYMER/ORGANOCLAY COMPOSITE
By Miss Busadee Homniam
Field of Study Petrochemistry and Polymer Science
Thesis Advisor Associate Professor Amorn Petsom, Ph.D.

Accepted by the Faculty of Science, Chulalongkorn University in Partial
Fullfillment of the Requirements for the Master's Degree

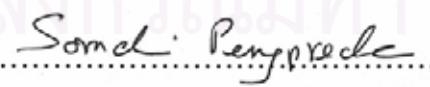

.....Dean of the Faculty of Science
(Professor Piamsak Menasveta, Ph.D.)

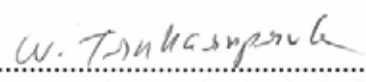
THESIS COMMITTEE


.....Chairman
(Professor Pattarapan Prasassarakich, Ph.D.)


.....Thesis Advisor
(Associate Professor Amorn Petsom, Ph.D.)


.....Member
(Professor Sophon Roengsumran, Ph.D.)


.....Member
(Associate Professor Somchai Pengprecha, Ph.D.)


.....Member
(Associate Professor Wimonrat Trakarnpruk, Ph.D.)

บุญฤดี หอมเนียม : สมบัติเชิงกลและเชิงความร้อนของคอมพอสิตลิกวิดคริสตัลพอลิเมอร์และออร์แกโนเคลย์. (MECHANICAL AND THERMAL PROPERTIES OF LIQUID CRYSTAL POLYMER/ORGANOCLAY COMPOSITE) อ. ที่ปรึกษา: รศ.ดร. อมร เพชรสม, 74 หน้า. ISBN 974-14-3386-7.

คอมพอสิตลิกวิดคริสตัลพอลิเมอร์และออร์แกโนเคลย์ เตรียมโดยวิธีหลอมเหลวแบบอินเทอร์คาเลชันของลิกวิดคริสตัลพอลิเมอร์และดินเหนียว ที่ปรับสภาพด้วยสารอินทรีย์ที่เป็นสารทำให้เกิดอินเทอร์คาเลชันมอลท์มอริลโลไนต์ โดยใช้สารลดแรงตึงผิวเฮกซะเดซิล ไตรเมทิลแอมโมเนียม โบรไมด์สำหรับการปรับสภาพผิวของมอลท์มอริลโลไนต์ให้เป็นออร์แกโนเคลย์ โดยการแลกเปลี่ยนไอออนระหว่างแคทไอออนในชั้นอินเทอร์เลเยอร์ของดินเหนียวกับแคทไอออนของสารลดแรงตึงผิว ผลการศึกษาการเลี้ยวเบนของรังสีเอ็กซ์และฟูเรียร์ทรานส์ฟอร์มอินฟราเรดสเปกโตรเมตรีพบว่าคอมพอสิตลิกวิดคริสตัลพอลิเมอร์และออร์แกโนเคลย์ที่เตรียมได้ แสดงให้เห็นว่ามีการแทรกตัวของลิกวิดคริสตัลพอลิเมอร์ในแต่ละชั้นของซิลิเกต การศึกษากำลังด้านทานจากการดึงพบว่าดินเหนียวมีผลต่อการเสริมแรงในคอมพอสิต ส่งผลให้มีค่ากำลังด้านทานจากการดึงที่ดีกว่าลิกวิดคริสตัลพอลิเมอร์บริสุทธิ์ การวิเคราะห์สมบัติทางความร้อนพบว่า การเติมดินเหนียวลงในลิกวิดคริสตัลพอลิเมอร์สามารถส่งผลให้การเสถียรต่อความร้อนดีขึ้น แต่สารลดแรงตึงผิวมีผลให้ค่าความเสถียรต่อความร้อนลดน้อยลง ผลการศึกษาจัดจำแนกระดับการหน่วงไฟของคอมพอสิตลิกวิดคริสตัลพอลิเมอร์และออร์แกโนเคลย์ปริมาณต่างๆพบว่าสามารถบรรลุนiveau ของยูแอล -94 ระดับวี-0

สถาบันวิทยบริการ
จุฬาลงกรณ์มหาวิทยาลัย

สาขาวิชา...ปีโทเคมีและวิทยาศาสตร์พอลิเมอร์...ลายมือชื่อนิสิต..... *Bisade H.*.....
ปีการศึกษา.....2549.....ลายมือชื่ออาจารย์ที่ปรึกษา..... *aw nsa*.....

4673417823 : MAJOR PETROCHEMISTRY AND POLYMER SCIENCE

KEY WORD: LIQUID CRYSTAL POLYMER / COMPOSITE /

ORGANOCLAY / MECHANICAL / THERMAL

**BUSADEE HOMNIAM : MECHANICAL AND THERMAL
PROPERTIES OF LIQUID CRYSTAL POLYMER/ORGANOCLAY
COMPOSITE. THESIS ADVISOR : ASSOC. PROF. AMORN
PETSOM, Ph.D., 74 pp. ISBN 974-14-3386-7.**

The liquid crystal polymer/organoclay composites were prepared by melt intercalation of liquid crystal polymer and montmorillonite clay organically modified with intercalating agent. The surfactant, hexadecyltrimethyl ammonium bromide was used to modify the montmorillonite surface to obtain the organoclay by ionic exchange between the interlayer cation and the surfactant cation. The resulting liquid crystal polymer intercalated into the organoclay was characterized by X-ray diffraction (XRD) and Fourier Transform Infrared spectrometry (FTIR). Tensile testing indicated that the reinforcement in the composites was more effective than pure polymer. The thermal stability and flammability of the liquid crystal polymer/organoclay composite were measured by thermogravimetric analysis (TGA) and UL-94, respectively. By adding organoclay, the thermal stability was improved but the surfactant decreased the thermal stability. The UL-94, V-0 rating was achieved for the liquid crystal polymer/organoclay composites with varying organoclay contents.

สถาบันวิทยบริการ
จุฬาลงกรณ์มหาวิทยาลัย

Field of Study.PETROCHEMISTRY AND POLYMER SCIENCE...Student's signature... *Busadee H.*

Academic Year.....2006.....Advisor's signature... *Amorn P.*

ACKNOWLEDGEMENTS

The author wishes to express her sincerest gratitude to her thesis advisor, Assoc. Prof. Dr. Amorn Petsom for his helpful suggestions, constant encouragement and guidance throughout the course of this thesis. To Prof. Dr. Pattarapan Prasassarakich, Prof. Dr. Sophon Roengsumran, Assoc. Prof. Dr. Somchai Pengprecha and Assoc. Prof. Dr. Wimonrat Trakarnpruk, the author is highly grateful for their valuable suggestions and advice as thesis examiners.

The author would like to thank Dr. Aticha Chaisuwan, Department of Chemistry, Faculty of Science, Chulalongkorn University for an access to the X-ray diffractometer and also extend to students and staff of Material Chemistry and Catalysis Research Unit for their kindly assistance and wonderful friendship. The author wishes to express her appreciation to Hitachi Global Storage Technologies(Thailand) Co., Ltd. for an access to SEM, FTIR and Mechanical testing equipment. The author also wishes to thank Polyplastic(Thailand) Co., Ltd. for the support in raw materials.

Finally, the author would like to express her appreciation and grateful to her family, encouragement and sincere care in every way throughout this study.



สถาบันวิทยบริการ
จุฬาลงกรณ์มหาวิทยาลัย

CONTENTS

	Page
ABSTRACT (in Thai).....	iv
ABSTRACT (in English).....	v
ACKNOWLEDGEMENTS.....	vi
CONTENTS.....	vii
LIST OF FIGURES.....	x
LIST OF TABLES.....	xii
LIST OF SCHEMES.....	xiii
LIST OF ABBREVIATIONS.....	xiv
CHAPTER I INTRODUCTION.....	1
CHAPTER II THEORY AND LITERATURE REVIEW.....	3
2.1 Liquid crystal polymer.....	3
2.1.1 Properties of thermoplastic liquid crystal polymer.....	5
2.1.2 Processing of liquid crystal polymer.....	6
2.2 Clay and Clay Mineral.....	7
2.2.1 Smectites.....	9
2.2.2 Montmorillonite.....	10
2.3 Organoclay.....	11
2.3.1 Organoclay structure and characterization.....	11
2.4 Polymer Nanocomposite.....	13
2.4.1 Preparation of polymer nanocomposite.....	15
2.4.2 Nanocomposite characterization.....	16
2.4.3 Nanocomposite properties.....	18
2.4.4 Application of polymer/clay nanocomposite.....	21
CHAPTER III EXPERIMENTAL.....	24
3.1 Materials.....	24

	Page
3.2 Equipments.....	24
3.3 Methodology.....	26
3.3.1 Preparation of organoclay and characterization.....	26
3.3.2 Preparation of liquid crystal polymer/organoclay Composite.....	28
3.3.3 Mechanical properties.....	30
3.3.4 Thermal property.....	30
3.3.5 Flammability properties.....	31
CHAPTER IV RESULTS AND DISCUSSION.....	32
4.1 Preparation of organoclay and characterization.....	32
4.4.1 The effect of surfactant chemistry of organoclay.....	33
4.1.1.1 XRD.....	34
4.1.1.2 FTIR.....	36
4.2 Preparation of Liquid crystal polymer/organoclay composite and Characterization.....	38
4.2.1 The dispersion of organoclay in Liquid crystal polymer/ organoclay composite.....	39
4.2.1.1 XRD.....	39
4.2.1.2 FTIR.....	41
4.2.2 Morphology of liquid crystal polymer/organoclay composite.....	45
4.3 Mechanical properties.....	48
4.4 Thermal property.....	50
4.5 Flammability properties.....	53
4.5.1 The vertical burning test.....	53
4.5.2 Limiting Oxygen Index.....	53
CHAPTER V CONCLUSION AND SUGGESTION FOR FUTURE WORK..	55
5.1 Conclusion.....	55
5.2 Suggestions for Future Work.....	56

	Page
REFERENCES	57
APPENDICES	61
VITAE	74



สถาบันวิทยบริการ
จุฬาลงกรณ์มหาวิทยาลัย

LIST OF FIGURES

	Page
Figure 2.1 Model structures of smectic and nematic rigid and semi-flexible main-chain LCPs and nematic side-chain LCPs where mesogens occur in pendant side chains.....	4
Figure 2.2 Tensile strength vs. degree of orientation.....	6
Figure 2.3 Structure of smectite clay.....	10
Figure 2.4 Orientations of alkylammonium ions in the galleries of layered silicates with different layer charge densities.....	13
Figure 2.5 Figure of different types of composite arising from the intercalation of layered silicates and polymers: (a) phase-separated microcomposite; (b) intercalated nanocomposite and (c) exfoliated nanocomposite.....	14
Figure 2.6 Schematic illustration of formation of hydrogen bonds in Nylon-6/MMT nanocomposite.....	19
Figure 4.1 Organic content of Na- Montmorillonite and organoclay.....	33
Figure 4.2 XRD pattern of Na-Montmorillonite.....	35
Figure 4.3 XRD pattern of HDTMAB/ Na-Montmorillonite (Organoclay).....	35
Figure 4.4 FTIR spectrum of Na- Montmorillonite.....	37
Figure 4.5 FTIR spectrum of HDTMAB-/ Na-Montmorillonite (Organoclay).	37
Figure 4.6 XRD pattern of the liquid crystal polymer/ organoclay composite.	39
Figure 4.7 FTIR spectrum of Pure Liquid crystal polymer.....	42
Figure 4.8 FTIR spectrum of Liquid crystal polymer with 1 %wt organoclay..	42
Figure 4.9 FTIR spectrum of Liquid crystal polymer with 3 %wt organoclay..	43
Figure 4.10 FTIR spectrum of Liquid crystal polymer with 5 %wt organoclay..	43
Figure 4.11 FTIR spectrum of Liquid crystal polymer with 7 %wt organoclay..	44
Figure 4.12 FTIR spectrum of Liquid crystal polymer with 10 %wt organoclay	44

Figure 4.13	Morphology of liquid crystal polymer/organoclay composite at various organoclay contents;(a) Pure LCP, (b) LCP/organoclay 1 %wt, (c) LCP/organoclay 3 %wt, (d) LCP/organoclay 5 %wt, (e) LCP/organoclay 7 %wt, (f) LCP/organoclay 10 %wt.....	47
Figure 4.14	Tensile strength and tensile modulus of liquid crystal polymer, liquid crystal polymer /organoclay composite and liquid crystal polymer with 30% glass fiber composite.....	49
Figure 4.15	Tensile strength and tensile modulus of liquid crystal polymer, liquid crystal polymer /organoclay composite and liquid crystal polymer with 30% glass fiber composite.....	49
Figure 4.16	Flexural strength and flexural modulus of liquid crystal polymer, liquid crystal polymer /organoclay composite and liquid crystal polymer with 30% glass fiber composite.....	50
Figure 4.17	Flexural strength and flexural modulus of liquid crystal polymer, liquid crystal polymer /organoclay composite and liquid crystal polymer with 30% glass fiber composite.....	50
Figure 4.18	TGA thermogram of liquid crystal polymer and liquid crystal polymer/organoclay composite.....	51

LIST OF TABLES

		Page
Table 2.1	Classification of phyllosilicates, example on clay minerals.....	8
Table 2.2	Chemical formula of clay in 2:1 phyllosilicates types.....	9
Table 3.1	Mould dimensions.....	28
Table 3.2	Composition of samples.....	28
Table 4.1	Elemental analysis of organoclay.....	33
Table 4.2	The interlayer spacing of Na- Montmorillonite and organoclay.....	34
Table 4.3	Infrared band assignment of Na-Montmorillonite , HDTMAB/ Na-Montmorillonite.....	38
Table 4.4	The interlayer spacing of organoclay and liquid crystal polymer/ organoclay.....	41
Table 4.5	Infrared band assignment of pure liquid crystal polymer and liquid crystal polymer/organoclay composite.....	45
Table 4.6	The tensile properties of LCP, LCP/organoclay composite and liquid crystal polymer with 30% glass fiber composite.....	48
Table 4.7	The flexural properties of LCP, LCP/organoclay composite and liquid crystal polymer with 30% glass fiber composite.....	48
Table 4.8	Weight loss percentages of liquid crystal polymer and liquid crystal polymer/organoclay composite.....	52
Table 4.9	UL-94 Classification of pure liquid crystal polymer and liquid crystal polymer/organoclay composite.....	53

จุฬาลงกรณ์มหาวิทยาลัย

LIST OF SCHEMES

	Page
Scheme 2.1 Liquid crystal polymer process diagram.....	5
Scheme 3.1 The diagram of preparation process for organoclay.....	27
Scheme 3.2 The diagram of preparation process for liquid crystal polymer/organoclay.....	29
Scheme 4.1 Hofmann elimination mechanism of quaternary ammonium salt...	52



สถาบันวิทยบริการ
จุฬาลงกรณ์มหาวิทยาลัย

LIST OF ABBREVIATIONS

LCP	Liquid Crystal Polymer
HDTMA	Hexadecyltrimethyl ammonium bromide
XRD	X-ray Diffraction
FTIR	Fourier Transform Infrared Spectroscopy
SEM	Scanning electron microscopy
AFM	Atomic force microscopy
TGA	Thermogravimetric analysis
LOI	Limiting Oxygen Index
UL-94	Underwriters Laboratory-94
CEC	Cation exchange capacity
Na-MMT	Sodium montmorillonite
LCP/organoclay 1 %wt	Composite of liquid crystal polymer with 1 %wt content of organoclay
LCP/organoclay 3 %wt	Composite of liquid crystal polymer with 3 %wt content of organoclay
LCP/organoclay 5 %wt	Composite of liquid crystal polymer with 5 %wt content of organoclay
LCP/organoclay 7 %wt	Composite of liquid crystal polymer with 7 %wt content of organoclay
LCP/organoclay 10 %wt	Composite of liquid crystal polymer with 10 %wt content of organoclay
LCP/ 30% glass fiber	Composite of liquid crystal polymer with 30 %wt content of glass fiber.

CHAPTER I

INTRODUCTION

1.1 The Statement of Problem

The polymer composite represent a radical alternative to conventional filled polymers or polymer blends. In reinforced plastics various inorganic materials are dispersed in the polymer which clay mineral have already been considered. The polymer composite often suffers from poor bonding between the polymer matrix and clay mineral due to clay mineral is immiscible with the hydrophobic polymer in pristine state. To match the polarity between the hydrophilic clay surface and the hydrophobic polymers, the clay mineral is modified with an alkylammonium salt by cation exchange to obtain organoclay. This results in a high surface area per volume, high aspect ratio, which become an alternative to current flame retardant, mechanical strength and gas barrier.

The liquid crystal polymer (LCP) is a thermoplastic polymer material with unique structural and physical properties. It contains rigid and flexible monomers that link to each other. When flowing in the liquid crystal state, rigid segments of the molecules align next to one another in the direction of shear flow. Once this orientation is formed, their direction and structure persist, even when LCP is cooled below the melting temperature. LCP offers a combination of electrical, thermal, mechanical and chemical properties.

1.2 Objective of research

The objective of this research is to prepare the liquid crystal polymer/ organoclay composite by melt processing and study on mechanical and thermal properties of the liquid crystal polymer/organoclay composite .

1.3 Scope of research

The organoclay was prepared from montmorillonite which was modified by hexadecyltrimethylammonium bromide (HDTMAB). This was done in order to improve bonding covalent of the liquid crystal polymer/organoclay composite. The dispersion of the organoclay was verified by XRD and FTIR. The morphology and topology were investigated by SEM. The mechanical property of composites was investigated by tensile and flexural testing. The thermal and flammability properties of composites were investigated by TGA, UL94 test and LOI. The liquid crystal polymer/organoclay composite was expected to exhibit better mechanical property, thermal and flammability stability than those of the pure liquid crystal polymer and commercial grade liquid crystal polymer reinforced with 30% glass fiber loading.



CHAPTER II

THEORY AND LITERATURE REVIEW

2.1 Liquid crystal polymer

A liquid crystal, or mesophase, is a state of matter between the liquid and crystal states. Liquid crystals are ordered like crystals but flow like liquids. The responsible anisotropic entities are known as mesogens. Liquid crystals are either thermotropic, which means that they are liquid crystalline in the temperature range between melt and solid states, or lyotropic, which means that they form liquid crystals in concentrated solutions. The temperature at which phase transition from liquid crystal to melt state occurs is called the isotropization (T_i) or clearing temperature (T_c).

Liquid crystals are classified according to the shape of the mesogens and the structure and appearance of the mesophases. Mesogens are either rod-like or disk-like and they are divided into three main classes: nematic, smectic, and cholesteric. The main classes are further divided into subgroups. The mesogenic units in a liquid crystalline polymer may be in the main chain or the side chain of the polymer. Polymeric liquid crystals are also classified according to their chemical structure and the conditions under which the LC state is formed. Main-chain LCPs may be either fully aromatic or built up of rigid mesogens and flexible spacers. In side-chain LCPs, the rigid mesogenic units usually are present in pendant side chains as shown in Figure 2.1 [1-3].

สถาบันวิทยบริการ
จุฬาลงกรณ์มหาวิทยาลัย

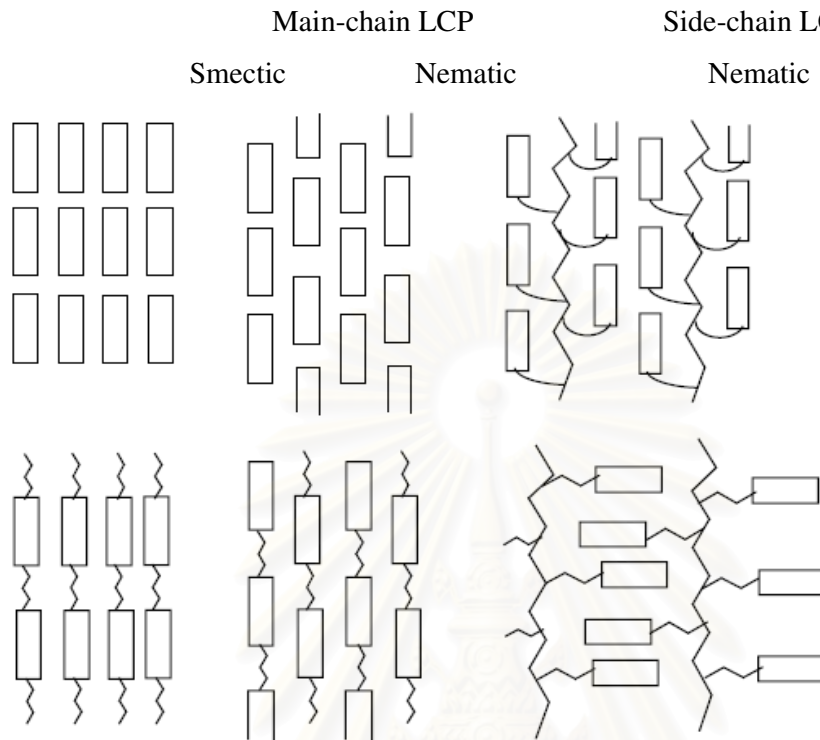


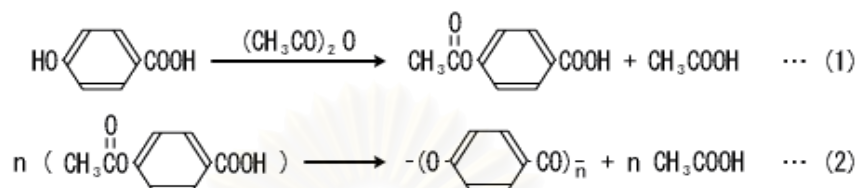
Figure 2.1 Model structures of smectic and nematic rigid and semi-flexible main-chain LCPs and nematic side-chain LCPs where mesogens occur in pendant side chains.

The main-chain LCPs are generally synthesized by polycondensation methods. Nematic structures are easy to produce since only large mesogens are required. Short mesogens connected by short flexible spacers are also possible. Smectic structures are usually obtained if rigid rod-like mesogens are present in periodic sequences or if mesogens of equal length are connected by large flexible spacers.

Radical polymerization of vinyl monomers is the most frequently used method for the synthesis of side-chain LCPs. The polymerization of suitable monomers and the reactions between mesogenic oligomers and flexible chains have also been utilized in the synthesis of side-chain LCPs [4].

Liquid crystal polymer, commercially grade ; Vectra A950 is comprised of acetylation of a monomer hydroxybenzoic acid with acetic anhydride (Formula 1) and polycondensation by acetic acid removal (Formula 2). In the acetylation process,

removal of acetic acid produced as a by-product from the system causes the equilibrium to shift to the right side of Formula 1 to complete the reaction as showed in Scheme 2.1.



Scheme 2.1 Liquid crystal polymer process diagram[4]

2.1.1 Properties of thermotropic liquid crystal polymer

Thermotropic LCPs, which are mainly random copolyesters and copolyesteramides, possess a unique combination of properties. The most significant characteristics are easy precision moldability, high outstanding dimensional stability and chemical resistance, low controllable coefficient of thermal expansion, low flammability and permeability, and exceptional strength, stiffness, and toughness [5].

In terms of commercial applications it is interesting to note that three classes of LCPs are emerging. The first is general-purpose LCPs that are exceptionally easy to process. These LCPs are possessed of high dimensional stability, molded-part repeatability, chemical resistance, good flame resistance, high strength, and good stiffness. The second class consists of LCPs that are more temperature-resistant and not quite as easy to process as the class I LCPs, but they have good dimensional stability, good chemical resistance, excellent flame resistance, and very good strength and stiffness properties. The third, lower-temperature/performance class consists of less expensive, less easily processed LCPs, which nevertheless have good dimensional stability, moderate chemical resistance, moderate flame resistance, good strength, and high stiffness [6].

2.1.2 Processing of liquid crystal polymer

The good mechanical strength and dimensional and thermal stability of thermotropic LCPs are based on their fibrous structure. Mechanical properties, particularly tensile strength and stiffness, depend upon the degree of orientation and particle size achieved in processing. As the level of elongational flow increases the mechanical properties improve to very high tensile modulus and strength. A compression molded unoriented LCP has similar mechanical properties to conventional isotropic polymers as showed in Figure 2.2 [7,8].

All processes that utilize flow to orient polymer molecules have the following three requirements: 1) the material must be in liquid or liquid crystalline state, something that can be achieved either by heat or by adding a suitable solvent to the pure polymer, 2) the fluid must be forced to flow in a manner that causes the polymer chains to orient, 3) the fluid must solidify, either through cooling of the pure polymer or through removal of solvent from the polymer solution [1].

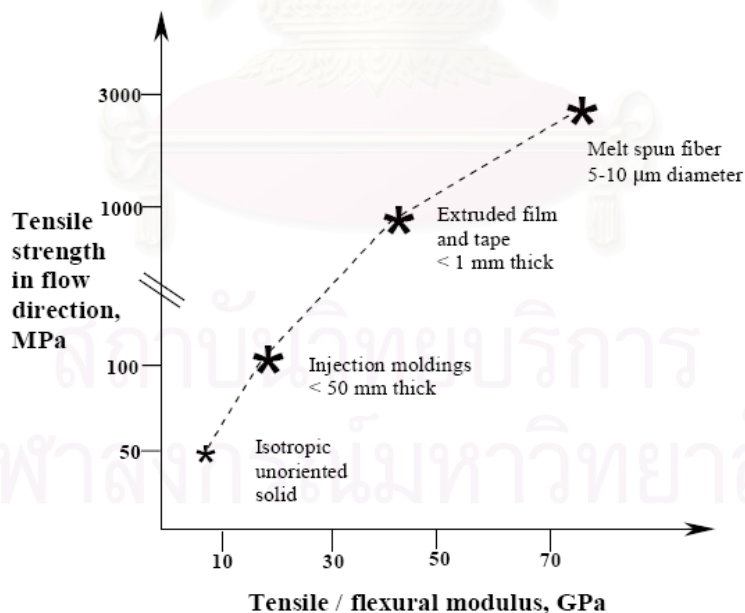


Figure 2.2 Tensile strength vs. degree of orientation [1]

2.2 Clay and Clay Mineral

Clay or layered silicate is a natural, earthy, fine grained material composed largely of a limited group of crystalline minerals known as the clay minerals. The clay minerals defined particular kind of crystallographic structure which are hydrous silicates containing tetrahedral silicate sheet and octahedral aluminum or magnesium sheet [9].

Clay minerals are called phyllosilicates were classified the layer structure into 1:1 and 2:1 families, as the main criterion for establishing divisions as showed in Table 2.1 [10] and the basic structural units in clays were defined as following.

(a) 1:1 type minerals

Non-swelling clays such as kaolinite consist of units of single sheet of silica tetrahedral between alumina octahedral sheets. These two sheets are 7 Å thick approximately.

(b) 2:1 type minerals

Swelling clays such as montmorillonite are composed of units made of two silica tetrahedral sheets between alumina octahedral sheet. These three sheets are 10 Å thick approximately.

Table 2.1 Classification of phyllosilicates, example on clay minerals

Layer type	Group	Subgroup	Species
1:1	Serpentine-Kaolin (z~0)	Serpentines (Tr)	Chrysotile, antigorite, lizardite, Berthierinc, odinite
		Kaolins (Di)	Kaolinite, dickite, nacrite, halloysite
2:1	Talc-Pyrophyllite (z~0)	Talc (Tr)	
		Pyrophyllite (Dr)	
	Smectite (z~0.2-0.6)	Smectites (Tr)	Saponite, hectorite
		Smectites (Dr)	Montmorillonite, beidellite, nontronite
	Vermiculite (z~0.6-0.9)	Vermiculite (Tr)	
		Vermiculite (Di)	
	Illite (0.6>z<0.9)	Illite (Tr)	
Illite (Di)		Illite, glauconite	
Mica (z~1.0)	Micas (Tr)	Biotite, phlogopite, lepidolite	
	Micas (Di)	Muscovite, paragonite	
Brittle mica (z~2.0)	Brittle micas	Margarite	
Chlorite (z variable)	Tr chlorites ^a (Tr)	Common name based on Fe ²⁺ , Mg ²⁺ , Mn ²⁺ , Ni ²⁺	
	Di chlorites (Di)	Donbassite	
	Tr chlorites (Di)	Sudolite, cookeite (Li)	
	Di chlorites (Tr)	No known examples	
2:1	Sepiolite-palygorsite	Inverted ribbons (with z variable)	

^a 2:1 layer first in name of chlorite; Tr = trioctahedral and Di = dioctahedral; z = charge per formula unit.

2.2.1 Smectites

Smectites are a group of clay minerals, belong to the same general family of 2:1 layered or phyllosilicates. Their crystal structure consists of layers made up of two tetrahedrally coordinated silicon atoms fused to an edge-shared octahedral sheet of either aluminum or magnesium hydroxide. The layer thickness is around 1 nm, and the lateral dimensions of these layers may vary from 30 nm to several microns or larger, depending on the particular layered silicate. Stacking of the layers leads to a regular Van Der Waals gap between the layers called the interlayer or gallery. Isomorphic substitution within the layers such as Al^{3+} replaced by Mg^{2+} or Fe^{2+} , or Mg^{2+} replaced by Li^{1+} generates negative charges that are counterbalanced by alkali and alkaline earth cations situated inside the galleries. This type of layered silicate is characterized by a moderate surface charge known as the cation exchange capacity (CEC), and generally expressed as milliequivalents per hundred grams of dry clay. This charge is not locally constant, but varies from layer to layer, and must be considered as an average value over the whole crystal [11].

The principle smectite are montmorillonite, beidellite and nontronite, all of which are dioctahedral 2:1 layer, and saponite, hectorite and saconite, which are trioctahedral [12]. Their chemical composition are shown in Table 2.2.

Table 2.2 Chemical formula of clay in 2:1 phyllosilicates types

Subgroup	Species	General formula
Dioctahedral smectictites	Montmorillonite	$M_{x/n}^{n+} \cdot y\text{H}_2\text{O}[\text{Al}_{4.0-x}\text{Mg}_x](\text{Si}_{8.0})\text{O}_{20}(\text{OH})_4$
	Beidellite	$M_{x/n}^{n+} \cdot y\text{H}_2\text{O}[\text{Al}_{4.0}](\text{Si}_{8.0-x}\text{Al}_x)\text{O}_{20}(\text{OH})_4$
	Nontronite	$M_{x/n}^{n+} \cdot y\text{H}_2\text{O}[\text{Fe}_{4.0}](\text{Si}_{8.0-x}\text{Al}_x)\text{O}_{20}(\text{OH})_4$
Trioctahedral smectictites	Saponite	$M_{x/n}^{n+} \cdot y\text{H}_2\text{O}[\text{Mg}_{6.0}](\text{Si}_{8.0-x}\text{Al}_x)\text{O}_{20}(\text{OH})_4$
	Hectorite	$M_{x/n}^{n+} \cdot y\text{H}_2\text{O}[\text{Mg}_{6.0-x}\text{Li}_x](\text{Si}_{8.0})\text{O}_{20}(\text{OH}, \text{Fe})_4$

The smectite clay structure consist of two tetrahedral layers of interconnected SiO_4 tetrahedral which enclose a central $\text{M}(\text{O},\text{OH})_6$ octahedral layer ($\text{M}=\text{Al}, \text{Fe}, \text{Mg}$

and others). The ability of smectite to absorb water is due in part to by the inherently small grain size of individual smectite crystals typically much less than $2\ \mu\text{m}$ and to the fact that individual sheets possess a negative surface charge which tends to attract polar molecules as showed in Figure 2.3 [13]. This negative charge is also responsible for another essential attribute of smectite, its ability to absorb positively charged ions from solutions, an attribute which, like adhesion, is also exploited commercially.

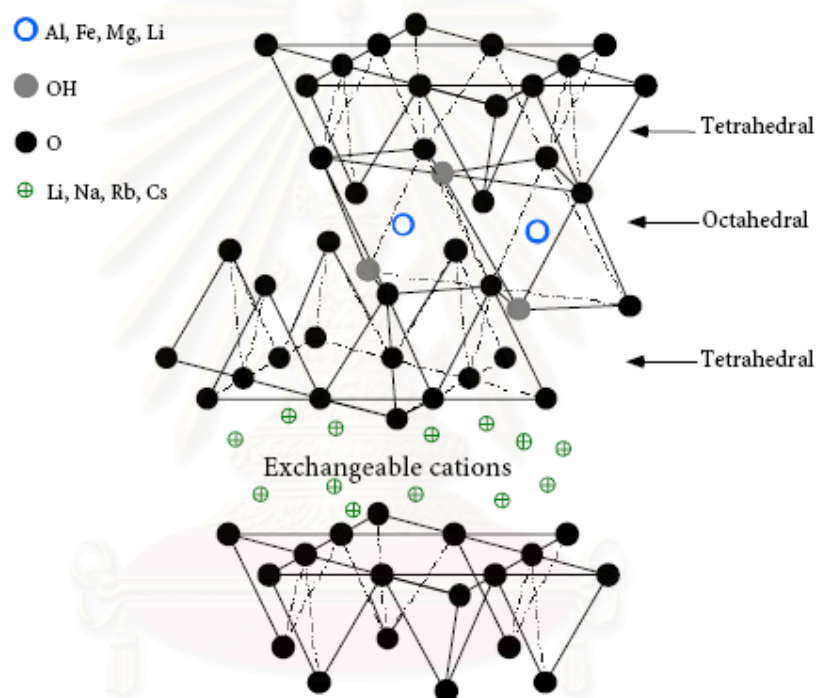


Figure 2.3 Structure of smectite clay

2.2.2 Montmorillonite

Montmorillonite is a member of the smectite family and the most commonly used layered silicates for the preparation of polymer layered silicate nanocomposites because it has the ability of the silicate particles to disperse into individual layers and the ability to fine-tune their surface chemistry through ion exchange reactions with organic and inorganic cations.

Montmorillonite's [water](#) content is variable and it increases greatly in volume when it absorbs water. Chemically it is hydrated sodium calcium aluminium magnesium silicate hydroxide $(\text{Na,Ca})_x(\text{Al,Mg})_2(\text{Si}_4\text{O}_{10})(\text{OH})_2 \cdot n\text{H}_2\text{O}$. Potassium, iron, and other cations are common substitutes, the exact ratio of cations varies with source of clays. Montmorillonite swells with the addition of water and ability to expand considerably more than other clays due to water penetrating the interlayer molecular spaces and concomitant adsorption. The amount of expansion is due largely to the type of exchangeable cation contained in the clay. The presence of sodium as the predominant exchangeable cation can result in the clay swelling to several times its original volume. The sodium montmorillonite has come to be used as the major constituent in ion exchange reactions to convert clay mineral to organophilic clay or organoclay [14].

2.3 Organoclay

The pristine clay can be modified from hydrophilic to organophilic making the intercalation of many engineering polymers possible. The modification can be done by (a) an adsorption of the organic molecule into an interlayer, (b) a covalently bonding of the surfactant to a free hydroxyl group on the clay surface and (c) an exchanging of an interlayer cation with a cation surfactant. This is resulting in a more compatible between organic molecule and the clay. The adsorption of the organic molecule often occurs via a complex formation between the organic molecule and the interlayer cation. The amount of the adsorbed molecule changes as a vapor pressure or temperature changes. The covalent bonded organoclay can be prepared by a condensation of a functionalized organo siloxane. Replacing an exchangeable interlayer cation by the cationic surfactant can carry out the exchange reaction to improve the strength of the interface between the inorganic and the polymer matrix.

2.3.1 Organoclay structure and characterization

The replacement of inorganic exchange cations by organic onium ions on the gallery surfaces of smectite clays not only serves to match the clay surface polarity

with the polarity of the polymer, but it also expands the clay galleries. This facilitates the penetration of the intercalation by either the polymer precursors or preformed polymer. Depending on the charge density of clay and the onium ion surfactant, different arrangements of the onium ions are possible. In general, the longer the surfactant chain length, and the higher the charge density of the clay, the further apart the clay layers will be forced. This is expected since both of these parameters contribute to increasing the volume occupied by the intragallery surfactant. Depending on the charge density of the clay, the onium ions may lie parallel to the clay surface as a monolayer, a lateral bilayer, a pseudo-trimolecular layer, or an inclined paraffin structure as illustrated in Figure 2.4. At very high charge densities, large surfactant ions can adopt lipid bilayer orientations in the clay galleries. The orientations of onium ion chains in organoclay were initially deduced based on infrared and XRD measurements [15]. More recent modeling experiments has provided further insights into the packing orientations of the alkyl chains in organically modified layered silicates [16]. Molecular dynamics (MD) simulations were used to study molecular properties such as density profiles, normal forces, chain configurations and trans-gauche conformer ratios. For the mono-, bi- and psuedo-trilayers with respective d -spacings of 13.2, 18.0 and 22.7 Å, a disordered liquid-like arrangement of chains was preferred in the gallery. In this disordered arrangement the chains do not remain flat, but instead, overlap and co-mingle with onium ions in opposing layers within the galleries. However, for the trilayer arrangement, the methylene groups are primarily found within a span of two layers and only occasionally do trans over gauche for the maximum surfactant chain length just before the system progresses to the next highest layering pattern. This is expected since the alkyl chains must be optimally packed under such dense surfactant concentrations. The MD simulation experiments have agreed well with experimental XRD data and FTIR spectroscopy for the stacked intragallery alkyl chains, however, the inclined paraffin association is not addressed experimentally seen for $< C_{15}$ surfactants with clays of CEC less than 1.2 meq/g and greater .

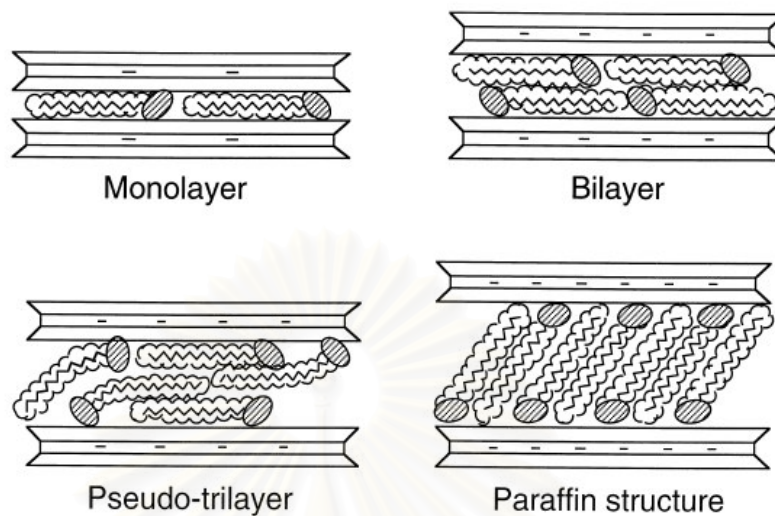


Figure 2.4 Orientations of alkylammonium ions in the galleries of layered silicates with different layer charge densities

Yurudu et al. [17] study the adsorbed surfactant affects the rheological and electrokinetic properties of sodium montmorillonite (NaMMT) dispersions. The degree of interaction between the surfactant and the NaMMT particles depends on the surfactant concentration in the suspension.

2.4 Polymer Nanocomposite

Nanocomposite are a combination of two or more phases containing different compositions or structures, where at least one of the phases is in the nanoscale regime. These materials exhibit behavior different from conventional composite materials with microscale structure due to small size of the structural unit and the high surface to volume ratio [18].

The use of organic and inorganic fillers is a common practice in the plastics industry to improve the mechanical properties of thermoplastic materials such as heat distortion temperature, hardness, toughness, stiffness and mold shrinkage or to decrease other properties such as gas permeability and often, material cost. The filler effect on the composite properties strongly depends on its shape, size, aggregation

state, surface characteristics and degree of dispersion. In general, the mechanical properties of a composite material with micron-sized fillers are inferior to the properties of a composite with nano-sized fillers. Physical properties such as surface smoothness and barrier properties cannot be achieved effectively using conventional, micron-sized fillers.

In general, layered silicates have layer thickness on the order of 1 nm and a very high aspect ratio (e.g. 10–1000). A few weight percent of layered silicates that are properly dispersed throughout the polymer matrix thus create much higher surface area for polymer/filler interaction as compared to conventional composites. Depending on the strength of interfacial interactions between the polymer matrix and layered silicate, Figure 2.5 showed three different types of polymer layered silicate nanocomposites are thermodynamically achievable [19].

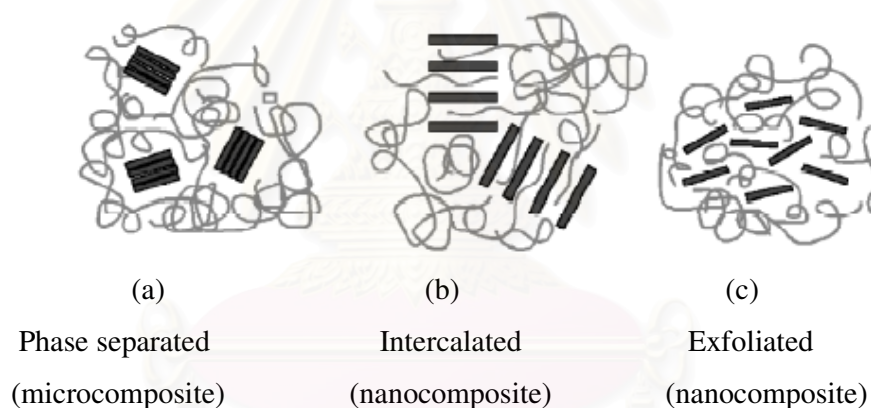


Figure 2.5 Figure of different types of composite arising from the intercalation of layered silicates and polymers: (a) phase-separated microcomposite; (b) intercalated nanocomposite and (c) exfoliated nanocomposite

Phase Separated Microcomposite

Phase separated microcomposite where the clay act as conventional filler. When the polymer is unable to intercalate between the silicate sheets, is obtained, whose properties stay in the same range as traditional microcomposites

Intercalated Nanocomposite

Intercalated structure in which a single extended polymer chain is intercalated between the layered silicates resulting in a well ordered multilayer morphology built up with alternating polymeric and inorganic layers.

Exfoliated Nanocomposite

The layered silicates are completely and uniformly dispersed in a continuous polymer matrix.

2.4.1 Preparation of polymer nanocomposite

Intercalation of polymers in layered hosts, such as layered silicates, has proven to be a successful approach to synthesize polymer layered silicates nanocomposite. The preparative methods are divided into three main groups according to the starting materials and processing techniques:

Intercalation of polymer or pre-polymer from solution

This is based on a solvent system in which the polymer or pre-polymer is soluble and the silicate layers are swellable. The layered silicate is first swollen in a solvent, such as water, chloroform, or toluene. When the polymer and layered silicate solutions are mixed, the polymer chains intercalate and displace the solvent within the interlayer of the silicate. Upon solvent removal, the intercalated structure remains, resulting in polymer layered silicate nanocomposite [20].

In situ intercalative polymerization method

In this method, the layered silicate is swollen within the liquid monomer or a monomer solution so the polymer formation can occur between the intercalated sheets. Polymerization can be initiated either by heat or radiation, by the diffusion of a suitable initiator, or by an organic initiator or catalyst fixed through cation exchange inside the interlayer before the swelling step.

Melt intercalation method

This method involves annealing, statically or under shear, a mixture of the polymer and organophilic modified layered silicate above the softening point of the polymer. This method has great advantages over either in situ intercalative polymerization or polymer solution intercalation. First, this method is environmentally benign due to the absence of organic solvents. Second, it is compatible with current industrial process, such as extrusion and injection molding. The melt intercalation method allows the use of polymers which were previously not suitable for in situ polymerization or solution intercalation.

2.4.2 Nanocomposite characterization

The structure of nanocomposite has typically been established five techniques for characterization. The most straightforward is X-ray diffraction (XRD) because it is easy to evaluate the spacing between the layered silicate and occasionally to study the kinetics of the polymer melt intercalation [21]. By monitoring the position, shape, and intensity of the basal reflections from the distributed the layered silicate, the nanocomposite structure (intercalated or exfoliated) may be identified. In an exfoliated nanocomposite, the extensive layer separation associated with the delamination of the original silicate layers in the polymer matrix results in the eventual disappearance of any coherent X-ray diffraction from the distributed silicate layers. On the other hand, for intercalated nanocomposites, the finite layer expansion associated with the polymer intercalation results in the appearance of a new basal reflection corresponding to the larger gallery height. However, the X-ray diffraction (XRD) offers a convenient method to determine the interlayer spacing of the layered silicate in the original layered silicates and in the intercalated nanocomposites (within 1–4 nm), some layered silicates initially do not exhibit well-defined basal reflections. Thus, peak broadening and intensity decreases are very difficult to study systematically. Therefore, conclusions concerning the mechanism of nanocomposites formation and their structure based solely on XRD patterns are only tentative. The second, FTIR is used to investigate the function group of the nanocomposite materials. The third, SEM is extensively used to verify the morphology and structure at surface

level. On the other hand, TEM allows a qualitative understanding of the internal structure, spatial distribution of the various phases, and views of the defect structure through direct visualization. The alternative method to observe atomic level features is the atomic force microscope (AFM) because it measures forces that are governed by the interaction potentials between atoms. Depending on the sample and tip material and the medium in between different interactions will be important. Always present are Van der Waals interaction and very short range repulsive interaction, which are caused by the quantum mechanical exclusion principle. Van der Waals forces are generally attractive (except for very rare cases) and can be sensed at distances of 10 Å and more [22].

X-Ray Diffraction

XRD is used to identify intercalated structures. In such nanocomposites, the repetitive multilayer structure is well preserved, allowing the interlayer spacing to be determined. The intercalation of the polymer chains usually increases the interlayer spacing, in comparison with the spacing of the organoclay used, leading to a shift of the diffraction peak towards lower angle values.

Angle and layer spacing values being related through the Bragg's relation:

$$\lambda = 2d \sin\theta$$

where λ corresponds to the wave length of the X-ray radiation used in the diffraction experiment, d the spacing between diffraction lattice planes and θ is the measured diffraction angle or glancing angle.

As far as exfoliated structure is concerned, no more diffraction peaks are visible in the XRD diffractograms either because of a much too large spacing between the layers (i.e. exceeding 8 nm in the case of ordered exfoliated structure) or because the nanocomposite lacks of order structure.

Fourier Transform Infrared Spectrometer

Fourier Transform Infrared Spectrometer (FTIR) is used to characterize the functional group of materials which is the most effective method for the analysis of organics compounds and identification of composition, since it required only small quantities of substances (min. size 10x10 µm) and allows the identification of solid,

liquid substances. When organic compounds are irradiated with IR light, specific wavelength light are absorbed. It leads IR spectrum characteristic of each material, same as fingerprint. So, it is useful to investigate the material characteristic.

Scanning Electron Microscopy

The scanning electron microscopy (SEM) is used to analyze the surface of specimens over a wide range of magnifications, a focused beam of electrons is either scanned across the surface of the specimen to form an image or stopped on a fixed location to performed one of a variety of spectrographic or analytical functions.

Secondary electrons and backscattered electrons are collected by their respective detectors and their signals are amplified. These electrons are used in imaging. Secondary electrons mainly provide surface topographic images while backscattered electrons can form images and supply atomic number information about the sample.

Atomic Force Microscopy

Atomic Force Microscopy (AFM) is used to characterize the nanocomposite morphology by a high-resolution imaging technique that can resolve features as small as an atomic lattice in the real space. It allows researchers to observe and manipulate molecular and atomic level features.

2.4.3 Nanocomposite properties

Nanocomposites consisting of a polymer and modified layered silicate frequently exhibit remarkably improved mechanical and materials properties when compared to those of pristine polymers containing a small amount (~5 %wt) of layered silicate. Improvements include a higher modulus, increased strength and heat resistance, decreased gas permeability and flammability, and increased biodegradability of biodegradable polymers. The main reason for these improved properties in nanocomposites is the stronger interfacial interaction between the matrix and layered silicate, compared with conventional filler-reinforced systems.

Mechanical properties

- Tensile properties

The tensile modulus of a polymeric material has been shown to be remarkably improved when nanocomposites are formed with layered silicates. Nylon-6 nanocomposites prepared through the in situ intercalative ring opening polymerization of 1-caprolactam, leading to the formation of exfoliated nanocomposites, exhibit a drastic increase in the tensile properties at rather low filler content. The main reason for the drastic improvement in tensile modulus in Nylon-6 nanocomposites is the strong interaction between matrix and silicate layers via formation of hydrogen bonds, as shown in Figure 2.6. In the case of nanocomposites, the extent of the improvement of the modulus depends directly upon the average length of the dispersed clay particles, and hence the aspect ratio. Moreover, the difference in the extent of exfoliation, as observed for Nylon-6 based nanocomposites synthesized by the in situ intercalative polymerization of 1-caprolactam using Na-MMT and various acids, strongly influenced the final modulus of the nanocomposites [23].

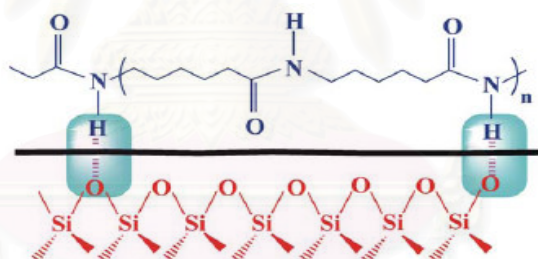


Figure 2.6 Schematic illustration of formation of hydrogen bonds in Nylon-6/MMT nanocomposite.

Liu X. et al.[24] reported the tensile properties of various PPCNs prepared with EM-MMT, a new type of co-intercalated MMT, The tensile strength of the PPCNs rapidly increase with increasing EM-MMT content from 0 to 5 %wt, but the trend is less pronounced when the clay content increases beyond 5 %wt. A similar trend is observed for the tensile modulus.

- Flexural properties

Sinha Ray et al. [25] reported the detailed measurement of flexural properties

of neat PLA and various PLACNs. They conducted flexural property measurements with injection-molded samples according to the ASTM D-790 method. The result of the flexural modulus, flexural strength, and distortion at break of neat PLA and various PLACNs measured at 25 °C. There was a significant increase in flexural modulus for PLACN4 when compared to that of neat PLA, followed by a much slower increase with increasing OMLS content, and a maximum at 21% for PLACN7. the flexural strength and distortion at break shows a remarkable increase with PLACN4, then gradually decreases with OMLS loading. According to the author, this behavior may be due to the high OMLS content, which leads to brittleness in the material.

Thermal stability

The thermal stability of polymeric materials is usually studied by thermogravimetric analysis (TGA). The weight loss due to the formation of volatile products after degradation at high temperature is monitored as a function of temperature. When the heating occurs under an inert gas flow, a non-oxidative degradation occurs, while the use of air or oxygen allows oxidative degradation of the samples. Zanetti et al. [26] conducted detailed TG analyses of nanocomposites based on EVA. The inorganic phase was fluorohectorite (FH) or MMT, both exchanged with octadecylammonium cation. They found that the deacylation of EVA in nanocomposites is accelerated, and may occur at temperatures lower than those for the pure polymer or corresponding microcomposite due to catalysis by the strongly acidic sites created by thermal decomposition of the silicate modifier. These sites are active when there is intimate contact between the polymer and the silicate. In air, the nanocomposite exhibits a significant delay in weight loss that may derive from the barrier effect caused by diffusion of both the volatile thermo-oxidation products to the gas and oxygen from the gas phase to the polymer.

The role of clay in the nanocomposite structure may be the main reason for the difference in TGA results of these systems compared to the previously reported systems. The clay acts as a heat barrier, which enhances the overall thermal stability of the system, as well as assist in the formation of char after thermal decomposition. In the early stages of thermal decomposition, the clay would shift the decomposition to higher temperature. After that, this heat barrier effect would result in a reverse thermal stability. In other words, the stacked silicate layers could hold accumulated heat that could be used as a heat source to

accelerate the decomposition process, in conjunction with the heat flow supplied by the outside heat source.

Flame retardancy

The Limiting oxygen index (LOI) methods and the vertical burning test (UL-94) are the most of conventional methods for studying the fire retardant properties of polymeric materials. Wang S. et al.[27] prepared flame retardant ABS/clay nanocomposites by melt blending ABS, organophilic montmorillonite and conventional flame retardants (DB and AO). Limiting oxygen index (LOI) and the vertical burning test (UL-94) showed improved properties in comparison to microcomposites. Adding 5 wt.% clay increases the LOI by about 0.5 units and ABS-DB/OMT achieves UL-94 V-0 grade while ABS-DB fails in the UL-94 test.

2.4.4 Application of polymer/clay nanocomposites

Polymer/clay nanocomposites offer tremendous improvement in a wide range of physical and engineering properties for polymers with low filler loading. This technology can now be applied commercially and has received great attention in recent year. The significant progress has been made in the development of synthetic methods, application to engineering polymers, and the investigation of major engineering properties. Polymer/clay nanocomposites are a typical example of nanotechnology. This class of material uses smectite-type clays, such as hectorite, montmorillonite, and synthetic mica, as fillers to enhance the properties of polymers. Smectite type clays have a layered structure. Each layer is constructed from tetrahedrally coordinated Si atoms fused into an edge shared octahedral plane of either $\text{Al}(\text{OH})_3$ or $\text{Mg}(\text{OH})_2$. According to the nature of the bonding between these atoms, the layers should exhibit excellent mechanical properties parallel to the layer direction. The principle used in clay/polymer nanocomposites is to separate not only clay aggregates but also individual silicate layers in a polymer, By doing this, the excellent mechanical properties of the individual clay layers can function effectively, while the number of reinforcing components also increases dramatically because each clay particle contains hundreds or thousands of layers. As a consequence, a wide range of engineering properties can be significantly improved with a low level of filler loading,

typically less than 5 %wt. At such a low loading level, polymers such as nylon-6 show an increase in Young's modulus of 103%, in tensile strength of 49%, and in heat distortion temperature of 146%[28]. Other improved physical and engineering properties include flame retardancy[29].

It is clear from this evidence that polymer/clay nanocomposites are a good demonstration of nanotechnology. By tailoring the clay structure in polymers on the nanometer scale, novel material properties have been found. Another interest in developing polymer/clay nanocomposites is that the technology can be applied immediately for commercial applications, while most other nanotechnologies are still in the concept and proving stage.

Kawasumi M. et al. [30] reported organoclay/liquid crystal nanocomposites that show a unique light scattering effect controlled by electric field, temperature change or shearing. Initially, a cell of the liquid crystalline composite (LCC) containing the organoclay scattered light strongly. However, upon the application of a low frequency electrical field, the cell became transparent. The liquid crystal showed a strong dielectric anisotropy, becoming aligned parallel to the electric field. This forced a similar alignment of the clay which minimized scattering and increased transparency.

Zeng Q.H. et al. [31] synthesized the nanocomposite by intercalation and in-situ polymerization. The montmorillonite (MMT) layers are completely dispersed in the polystyrene (PS). The resulting nanocomposite displayed higher thermal stability compared with pure PS. This improved property was attributed to the nanoscale dispersion of high aspect ratio of MMT layers as well as the similar structure between the alkyl chain in organo-MMT and styrene monomer.

Wang M.Z. et al. [32] studied the effect of monoalkyl- and dialkyl-imidazolium surfactants which used to prepare organically modified montmorillonites with markedly improved thermal stability in comparison with their alkyl-ammonium equivalents. The thermal stability affords the opportunity to form syndiotactic polystyrene (s-PS)/imidazolium-montmorillonite nanocomposites under static melt-intercalation condition. The syndiotactic polystyrene (s-PS) exhibited an improvement in the thermal stability in comparison with neat s-PS, and the β -crystal form of s-PS became dominant.

Lee M.W. et al. [33] studied the formation of LCP fibrils under shear flow, extensional flow and the effect of adding fillers. The addition of the fillers has increased the viscous force of the system and improved the deformability of the LCP phase. Consequently, LCP fibrils can be developed using a single injection moulding process. The nanosilica coupled with the in-situ reinforcements that was evolved from the addition of fillers was found to enhance the properties of the filler/LCP/thermoplastic composites.

Wang S. et al. [27] prepared flame retardant ABS/clay nanocomposites by melt blending ABS, organophilic montmorillonite and conventional flame retardants (DB and AO). Cone calorimeter experiments, UL-94 and LOI tests show that the nanocomposites were superior to that of conventional flame retardant microcomposites.

Zhoa C. et al. [34] prepared PE/clay nanocomposites by melt intercalation method. Mechanical testing, thermal stability and flammability indicated that the reinforcement in the nanocomposites were more effective than that in their conventional counterparts.

Ratna D. et al. [35] prepared poly(ethylene oxide) (PEO)/clay nanocomposites by a solution intercalation method. Improvement in tensile properties in all respect was observed for nanocomposites with optimum clay content (12.5 %wt). Crystallinity in general tends to decrease with the addition of clay, which is beneficial for its application as electrolyte in association with alkali metal ions.

CHAPTER III

EXPERIMENTAL

3.1 Materials

Liquid Crystal Polymer (LCP), a commercial grade VECTRA A950, was supported as pellets by Polyplastics (Bangkok, Thailand) and used as composite matrix resin. The original purified sodium montmorillonite (Na-MMT) with a cation exchange capacity of 122 meq/ 100 g of clay and average particle sizes $< 2 \mu\text{m}$ was kindly provided by Volclay Siam (Rayong, Thailand).

The intercalating agent was used for modification of Na-MMT. It was the reactive hexadecyltrimethylammonium bromide 99%, MW 364.45, chemical formula $\text{C}_{19}\text{H}_{42}\text{BrN}$ was of analytical grade quality obtained from ACROS. The excess bromide ion was detected by silver nitrate (AgNO_3) solution.

3.2 Equipments

Fourier Transform Infrared Spectrometry (FTIR)

Fourier transform infrared spectrum were obtained on Jasco Model 610 at room temperature by using a potassium bromide (KBr) beamsplitter and a JascoPlan FTIR microscope. The FTIR microscope was equipped with a narrow band liquid nitrogen cooled MCT (mercury cadmium telluride) detector allowing spectra to be obtained between 4000 and 700 cm^{-1} at a resolution of 4.0 cm^{-1} and the scanning speed was 4.0 mm/sec .

X- ray Diffractometer (XRD)

X – ray diffractometer was performed on Rigaku I/max diffractometer using $\text{Cu K}\alpha$ radiation ($\lambda = 1.5406 \text{ \AA}$) at a generated voltage of 40 kV and current of 20 mA at room temperature. The diffractograms were scanned from 2° to 30° in the 2θ range in 0.02 degree /step with a scanning rate of $8^\circ / \text{min}$.

Particle size Analyzer

The particle size analysis was investigated on Mastersizer S Ver. 2.19 in medium DI water and disperse with 0.1% Sodium hexametaphosphate by 10 min. sonicated in ultrasonic bath before analysis and stirred deionized (DI) water during measurement.

CHNS/O Analyzer

The elemental analysis of organoclay was carried out by Perkin Elmer PE2400 SeriesII.

Scanning Electron Microscopy (SEM)

The morphology of the tensile fractured was investigated on Hitachi S-4200 scanning electron microscope with an accelerating voltage of 5.0 kV. A thin layer of gold was sputtered on the surface of the specimens for electrical conductivity.

Universal Testing Machine

Tensile and flexural tests were conducted on an Instron universal material testing machine Model 4502. Tensile strength was determined at a crosshead speed of 50 mm/min, and the results reported here are the averages of five successful tests. Flexural properties were measured at a crosshead speed of 2 mm/min, and the results reported here are the averages of five successful tests.

Thermal Gravimetric Analyzer

The thermal stability was tested by thermogravimetric analysis (TGA) using Mettler Toledo TGA/SDTA 851° at a scan rate of 20°C/min under nitrogen flow from 30°C to 600°C and then change to under oxygen until the temperature reaches 850°C.

Vertical Burning Test

Flammability was obtained by vertical UL-94 classification. The specimens size was 120 mm long by 10.3 mm width and 3.9 mm thickness.

Limiting Oxygen Index (LOI)

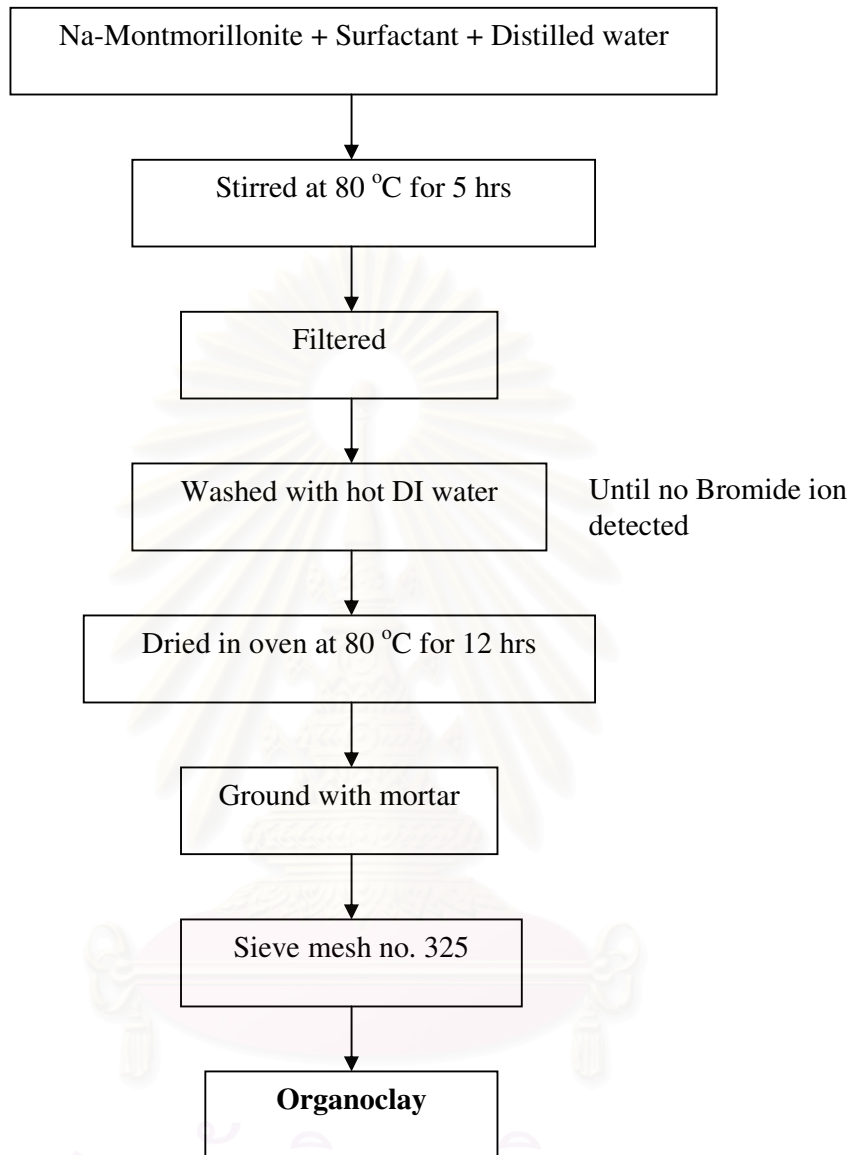
The limiting oxygen index was measured on LOI instrument. The LOI value was taken as the minimum percentages of oxygen required in a nitrogen-oxygen atmosphere, surrounding the samples, to maintain its combustion for at least 30 s after ignition.

3.3 Methodology

3.3.1 Preparation of organoclay and characterization

The original purified Na- Montmorillonite (33 g) was gradually added to a solution of quaternary ammonium salt by using hexadecyltrimethyl ammonium bromide (C16) at concentration 2.7 mmol in distilled water (667 ml) at 80 °C and vigorously stirred for 5 hrs. The white precipitate was repeatedly washed by hot deionized water to remove the excess of hexadecyltrimethyl ammonium bromide (C16) until no bromide ion was detected with 0.1 AgNO₃ solution. The solution was filtered and placed in a vacuum oven at 80 °C for 12 hrs for drying. The dried cake was ground with mortar then passed through sieve mesh no. 325 and the obtained organoclay was characterized by FTIR, XRD, Particle size Analyzer and Elemental Analyzer.

สถาบันวิทยบริการ
จุฬาลงกรณ์มหาวิทยาลัย



Scheme 3.1 The diagram of preparation process for organoclay [27]

3.3.2 Preparation of liquid crystal polymer/organoclay composite

The liquid crystal polymer, a commercial grade VECTRA A950 and the organoclay were dried at 60 °C for 24 hrs prior to use. Then the liquid crystal polymer and organoclay were pre-mixed in a dry mixer then melt compounded in a co-rotating twin screw extruder (Collin, ZK 25) with 30 mm diameter (Φ) and longitudinal per diameter (L/Φ) at 24. The barrel temperature was maintained at 290 °C and the screw speed was 200 rpm. The obtained liquid crystal polymer/ organoclay composites contain 1, 3, 5, 7, 10 %wt organoclay loading respectively.

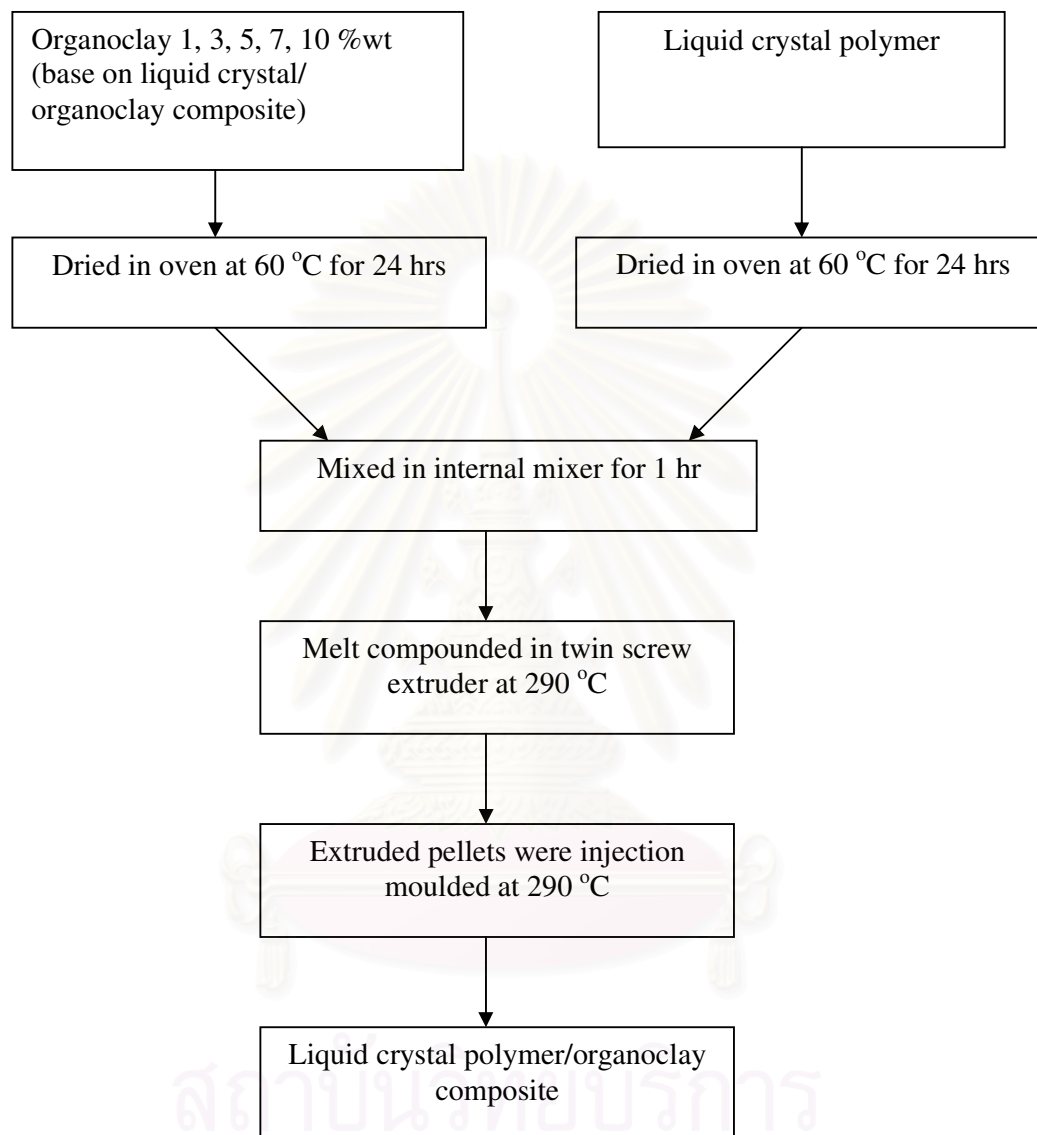
The extruded pellets were injection-moulded into the standard specimens according to the ASTM test method. The barrel temperature was 290 °C, and injection pressure was 80 Mpa. After moulding, the specimens were placed in a desiccator for 48 hrs prior to the test. The summarized procedure for preparation of liquid crystal polymer/organoclay composite is shown in Table 3.1. The composition of samples is shown in Table 3.2.

Table 3.1 Mould dimensions

Shape	Properties	Mould dimension (mm) length x width x thickness
Dog Bone	Tensile	153 x 10.3 x 3.9
Bar	Flexural	64 x 13 x 3.4

Table 3.2 Composition of samples

Sample	Liquid crystal polymer(LCP)	Organoclay (%wt)
LCP	100	0
LCP/ organoclay	99	1
LCP/ organoclay	97	3
LCP/ organoclay	95	5
LCP/ organoclay	93	7
LCP/ organoclay	90	10



Scheme 3.2 The diagram of preparation process for liquid crystal polymer/organoclay composite

3.3.3 Mechanical properties

To investigate mechanical properties of the liquid crystal polymer/organoclay composite.

Tensile properties

Tensile strength and modulus at break were measured by using the Instron universal material testing machine Model 4502. Tensile properties were determined at a crosshead speed of 50 mm/min, and the results reported here are the averages of five successful tests. The test specimens are aged at 21 °C and 51% humidity for 48 hrs before the test.

Flexural properties

Flexural strength and modulus at break were measured by using the Instron universal material testing machine Model 4502. Flexural properties were measured at a crosshead speed of 2 mm/min, and the results reported here are the averages of five successful tests. The test specimens are aged at 21 °C and 51% humidity for 48 hrs before the test.

3.3.4 Thermal property

Thermal stability

The thermal stability was tested by thermogravimetric analysis(TGA) using Mettler Toledo TGA/DSTA 851^e at a scan rate of 20°C/min under nitrogen flow from 30°C to the temperature 600°C and then change to under oxygen until the temperature reach 850°C. The samples were tested and revealed the decomposition temperature of the liquid crystal polymer/organoclay composite.

3.3.5 Flammability property

Vertical burning test (UL-94)

Flame retardant of the liquid crystal polymer/organoclay composite was evaluated by the vertical burning test (UL-94) that revealed a qualitative classification of the samples. All specimens were to be cut from dog bone shape to the necessary form. After any cutting operation, care to be taken to remove all dust and any particles from the surface. Fabrication of test specimens were cut according to dimension size 120 mm long by 10.3 mm width and 3.9 mm thickness.

Limiting Oxygen Index (LOI)

The LOI is the one of the methods for studying the flame retardant properties. The result of LOI revealed the minimum concentration of oxygen, expressed as volume percent, in a mixture of oxygen and nitrogen that would just support flaming combustion of a material initially at room temperature.

CHAPTER IV

RESULT AND DISCUSSION

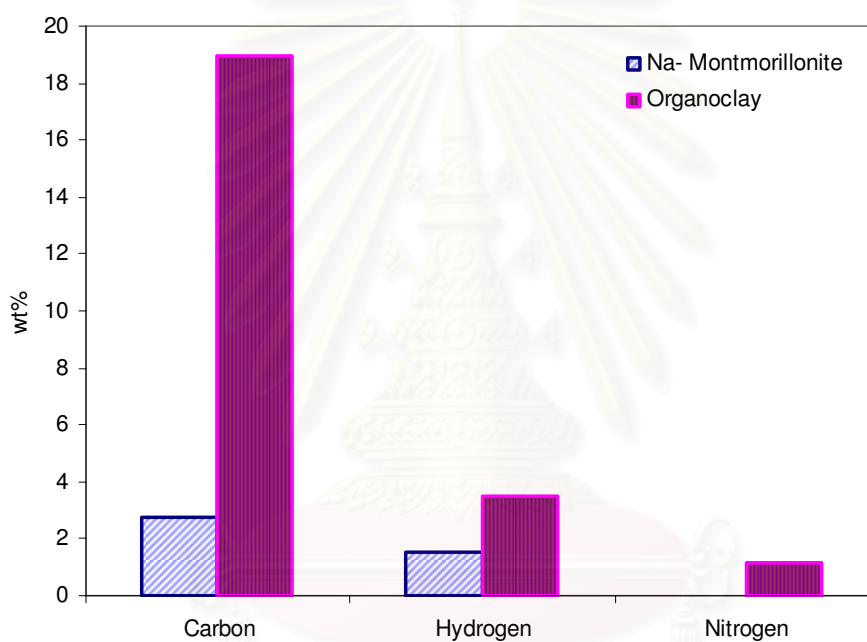
4.1 Preparation of organoclay and characterization

Typical synthesis of the liquid crystal polymer/organoclay composite involves organically modification of clay with the alkylammonium cation and intercalation of a suitable monomer followed by ion exchange reaction. The role of alkylammonium cation is to improve penetration of the organophilic monomers into the clay interlayer region and the role of the monomer is to promote dispersion of the clay interlayer distance. Since the increased basal spacing arises from the expansion of the interlayer region to accommodate pristine clay, the intercalation process can be distinguished from the difference in basal spacing.

The Na- Montmorillonite is used as a template for the organoclay preparation. The hexadecyltrimethyl ammonium bromide is used as a quaternary ammonium salt for ion exchanged reaction. The suspension was stirred until an equilibrium exchange reaction was reached. Excess bromide ion was washed several times with hot deionized water until no white precipitation of silver bromide was detected by silver nitrate solution. The organoclay was dried and ground with mortar then pass sieve mesh no. 325, the lateral dimensions of these stacked silicate layers with average particle sizes of 20 μm and vary from 2 μm to 41 μm while the silicate layers have a high aspect ratio and each one is approximately 1 nm thick which will be investigated by XRD. The organic contents (%wt) of organoclay was investigated by elemental analysis. According to Table 4.1 and Figure 4.1, the increased organic contents such as carbon (%wt), hydrogen (%wt) and nitrogen (%wt) due to the alkylammonium cations were shown to provide organic functional groups into the silicate layers.

Table 4.1 Elemental analysis of organoclay

Sample	%Carbon	%Hydrogen	%Nitrogen
Na-Montmorillonite	2.75	1.54	0
Organoclay	18.93	3.50	1.2

**Figure 4.1** Organic content of Na- Montmorillonite and organoclay

4.1.1 The effect of surfactant chemistry of organoclay

The intercalation of silicate layer was investigated by X-ray diffraction (XRD) and Fourier transform infrared spectrometry (FTIR).

4.1.1.1 XRD

The basal spacing (d_{001}) from XRD measurement was calculated from Bragg's law: $d = \lambda / (2 \sin \theta)$ at peak positions. Figure 4.2 shows the XRD pattern of pristine Na-Montmorillonite and HDTMAB/ Na-Montmorillonite (organoclay) in the range of the diffraction angle 2θ from 2° to 30° . The peaks of Na-Montmorillonite occurred at $2\theta = 7.000^\circ, 19.601^\circ, 20.950^\circ, 26.681^\circ, 28.558^\circ$ and 29.465° with d-spacing of 1.26 nm, 0.45 nm, 0.42 nm, 0.33 nm, 0.31 nm and 0.30 nm., respectively. In order to determine the change in basal spacing, d_{001} of 1.26 nm at (001) diffraction peak $2\theta = 7.000^\circ$ for Na-Montmorillonite layer was compared with the corresponding values of HDTMAB/ Na-Montmorillonite. It was noted that (001) peak at 7.000° of Na-montmorillonite shifted to 4.101° in HDTMAB/ Na-Montmorillonite with corresponding increase in d-spacing from 1.26 nm to 2.15 nm respectively as shown in Figure 4.3. The increase in interlayer spacing of HDTMAB/ Na-Montmorillonite was attributed to the surfactant used. Alkylammonium modification is essential for making the clay particles organophilic and also for increasing their d-spacing. The clay sheets are bound with in-plane covalent bonds and therefore, their crystal structure is stable, but clay layers are held loosely with Van der Waals bonds and therefore, expansion of interlayers is commonly seen when organic molecules are introduced between the layers [17].

Table 4.2 The interlayer spacing of Na- Montmorillonite and organoclay

Types	Angle ($^\circ 2\theta$)	Interlayer spacing (nm)
Na- Montmorillonite	7.000	1.26
Organoclay	4.101	2.15

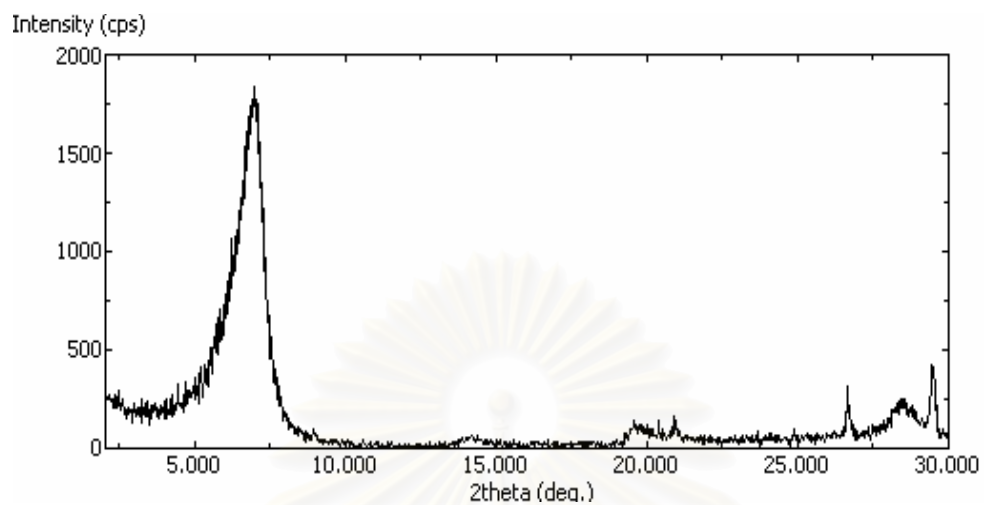


Figure 4.2 XRD pattern of Na-Montmorillonite

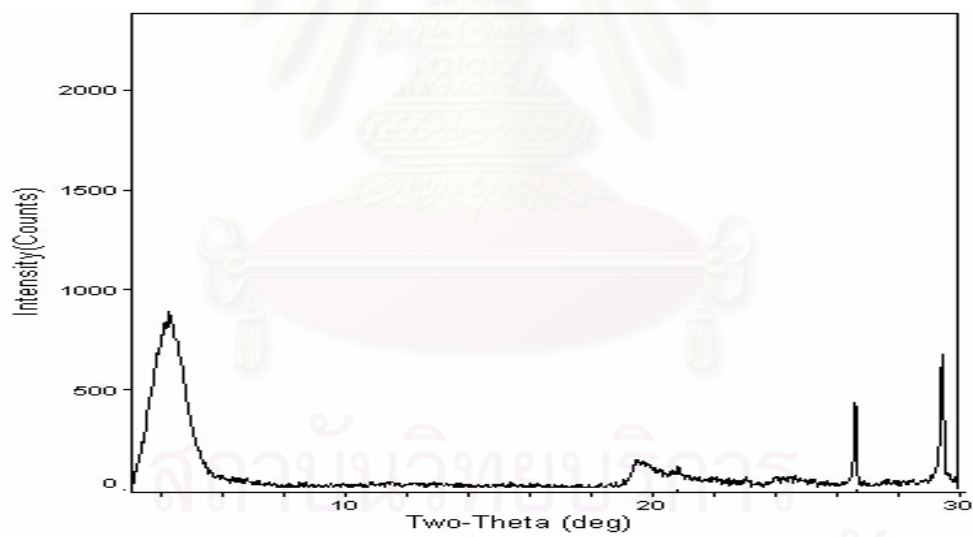


Figure 4.3 XRD pattern of HDTMAB/ Na-Montmorillonite (Organoclay)

4.1.1.2 FTIR

The absorption of infrared radiation by clays was recorded over a range 4000 to 700 cm^{-1} . The Na-Montmorillonite showed characteristic smectitic clay mineral peaks at 881, 1004, 1454, 1643, 3415, 3625 cm^{-1} and characteristic absorption bands were assigned to be the O-H bending band, Si-O-Si stretching band, C-H bending band, H-O-H bending of water band and O-H stretching of water band, respectively. The Na-Montmorillonite showed no intense peaks corresponding to organic matter of alkylammonium cation at 1467, 2850 and 2923 cm^{-1} which absorption bands were assigned to the peaks of CH_2 plane scissoring band, CH_2 symmetric stretching band, CH_2 asymmetric stretching band, respectively [36].

The organoclay also showed the characteristic peaks of clay minerals, albeit of low intensity. This is an indicative of the organophilic character of the clay. The organic matter peaks at 1467 cm^{-1} was sharper than those of the natural clay (Na-Montmorillonite) and 2850 and 2923 cm^{-1} were observed in organoclay but not observed in the natural clay (Na-Montmorillonite). These bands confirmed the alkylammonium intercalation in the interlayer galleries of the clay mineral, and the lower intensity of the characteristic clay mineral peaks indicated the organophilic nature of the treated clay.

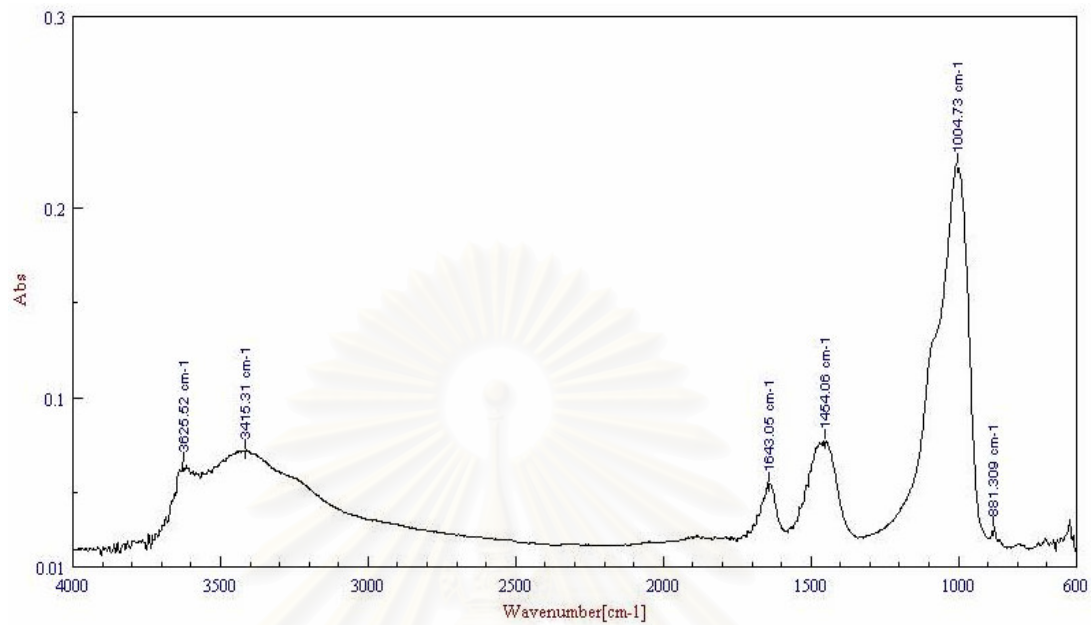


Figure 4.4 FTIR spectrum of Na- Montmorillonite

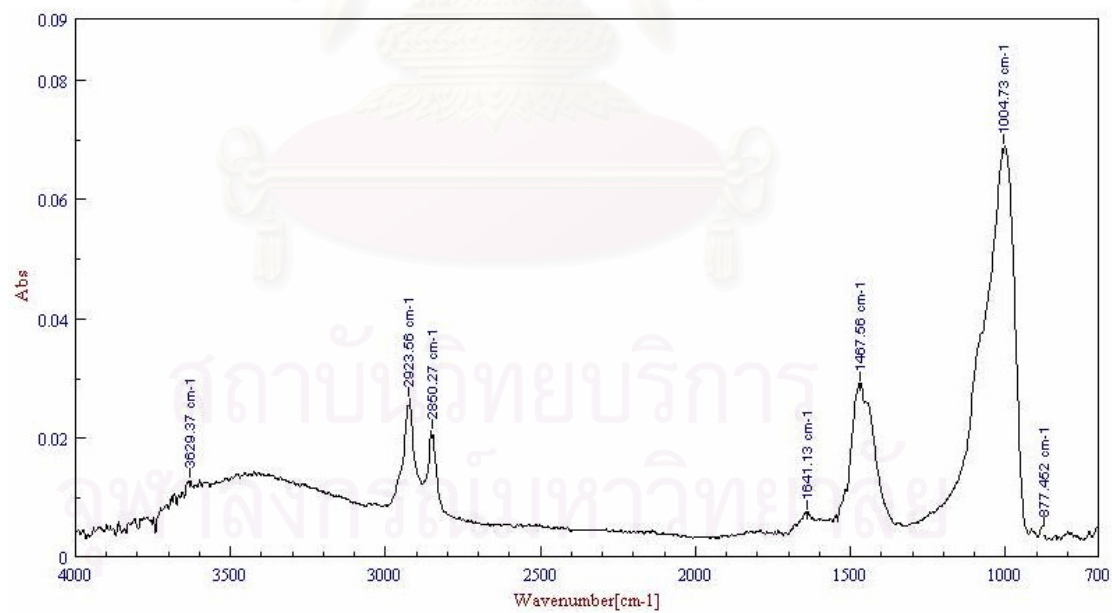


Figure 4.5 FTIR spectrum of HDTMAB-/ Na-Montmorillonite (Organoclay)

Table 4.3 Infrared band assignment of Na-Montmorillonite , HDTMAB/
Na-Montmorillonite

Sample	Frequency cm^{-1}	Band assignment
Na-Montmorillonite	3625,3414	O-H stretching of water
	1643	H-O-H bending of water
	1454	C-H bending
	1004	Si-O-Si stretching
	881	O-H bending
HDTMAB-/ Na-Montmorillonite	3629	O-H stretching of water
	2923	CH_2 asymmetric stretching
	2850	CH_2 symmetric stretching
	1641	H-O-H bending
	1467	CH_2 plane scissoring
	1004	Si-O-Si stretching
	877	O-H bending

4.2 Preparation of liquid crystal polymer/organoclay composite and characterization

The liquid crystal polymer/organoclay composite was prepared by twin screw extruder and injection moulding and the reactive intercalating agent was directly used to modified the Na- montmorillonite clay, so that the chemical reaction with hydroxyl groups at the edge of clay layers and the interlayer ion exchange were carried out. The obtained liquid crystal polymer/organoclay composites contain 1, 3, 5, 7, 10 %wt organoclay loading respectively.

4.2.1 The dispersion of organoclay in liquid crystal polymer/organoclay composite

The dispersion of organoclay in the liquid crystal polymer was verified by X-ray diffraction (XRD) and Fourier Transform Infrared (FTIR). From the basal spacing of the liquid crystal polymer/organoclay composite, it was expected to obtain the evidence of intercalated and/or exfoliated structures. On the other hand, FTIR provided the evidences of the formation of polymer.

4.2.1.1 XRD

The polarity of clay mainly consist in its interlayer surface. Through the ion exchange with common alkyl ammonium, the surface of the clay would change from hydrophilic to organophilic, and can be used to fabricate most of liquid crystal polymer/organoclay composite. But for non-polar liquid crystal polymer, the hydroxyl groups at the edge of clay layers impair the formation of composite. Therefore, a reactive intercalating agent was used for the modification of clay surface. The molecule of the reactive intercalating agent, hexadecyltrimethyl ammonium bromide contains both exchangeable cations that act as ammonium cations to replace the interlayer Na^+ and reactive methoxysilane groups that could react with hydroxyl groups at edges of clay layers. The lattice reaction could further reduce the interlayer attraction and improve the wettability between liquid crystal polymer and organoclay and ultimately enhance the intercalation of liquid crystal polymer into interlayers of clay.

The organoclay showed a diffraction peak at $2\theta = 4.101^\circ$, interlayer spacing 2.15 nm corresponding to (001) diffraction peak. The XRD patterns of the liquid crystal polymer/organoclay composite with different organoclay loading content are shown in Figure 4.6. The interlayer spacing of liquid crystal polymer/organoclay composite with 3, 5, 7, 10 %wt content is not significant difference because the quantity of organoclay did not affect to the interlayer spacing but liquid crystal polymer/organoclay composite with 3, 5, 7, 10 %wt content showed that the

interlayer spacing was increased more than 2.15 nm when compared with the organoclay which indicated the increase in d-spacing of the clay layers and occurrence of intercalation of the liquid crystal polymer chains. However, it is clearly observed in the pattern of liquid crystal polymer/organoclay composite with 1 %wt content of organoclay, that the interlayer spacing has been disappeared which indicates the exfoliated structure. It is also possible that the interlayer spacing is larger than the detection limit of the XRD used in this study, at 8.8 nm.

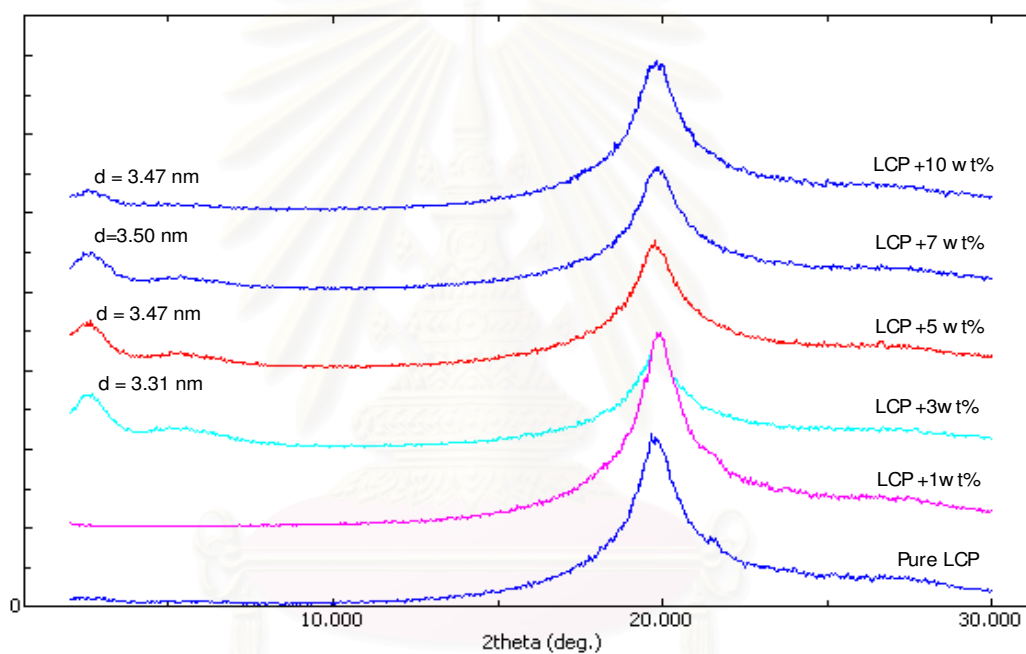


Figure 4.6 XRD patterns of the liquid crystal polymer/organoclay composite

Table 4.4 The interlayer spacing of organoclay and liquid crystal polymer/organoclay

Types	Angle ($^{\circ}2\theta$)	Interlayer spacing (nm)
Organoclay	4.101	2.15
LCP	-	-
LCP/organoclay 1 %wt	-	-
LCP/organoclay 3 %wt	2.662	3.31
LCP/organoclay 5 %wt	2.541	3.47
LCP/organoclay 7 %wt	2.517	3.50
LCP/organoclay 10 %wt	2.542	3.47

4.2.1.2 FTIR

Further evidence for the intercalation can be obtained from the FTIR spectrum recorded for the extracted liquid crystal polymer/organoclay composite. The FTIR spectra are shown in Figures 4.7-4.12. The liquid crystal polymer showed characteristic peaks and absorption bands of OH out-of-plane bending of aromatic ring vibrations at 757, 888, 931 cm^{-1} , C-O stretching vibrations at 1013, 1051, 1157, 1181, 1201, 1258 cm^{-1} , C=C stretching vibrations at 1414, 1472, 1506, 1600, 1630 cm^{-1} , C=O stretching vibrations at 1738 cm^{-1} , O-H stretching vibrations at 3080 cm^{-1} . The absorption bands related to organoclay are also found, such as CH_2 symmetric stretching band vibrations at 2854 cm^{-1} and CH_2 asymmetric stretching band vibrations at 2925 cm^{-1} in the liquid crystal polymer with organoclay loading at 3, 5, 7, 10 %wt. The existence of liquid crystal polymer and organoclay characteristic peaks in fully extracted composite is ascribed to the delamination of organoclay layers within the polymer matrix [36].

For liquid crystal polymer with 1 %wt organoclay, it was not shown the characteristic peaks and absorption bands at 2854 cm^{-1} and 2925 cm^{-1} which are the characteristic peaks and absorption bands of organoclay. This suggested that there was no interaction between organoclay and the liquid crystal polymer.

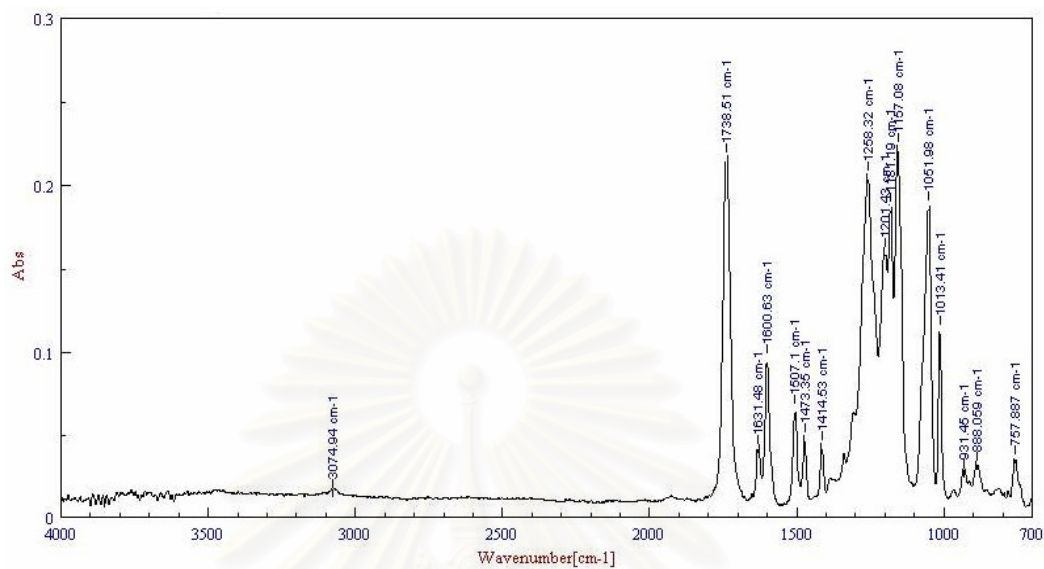


Figure 4.7 FTIR spectrum of pure liquid crystal polymer

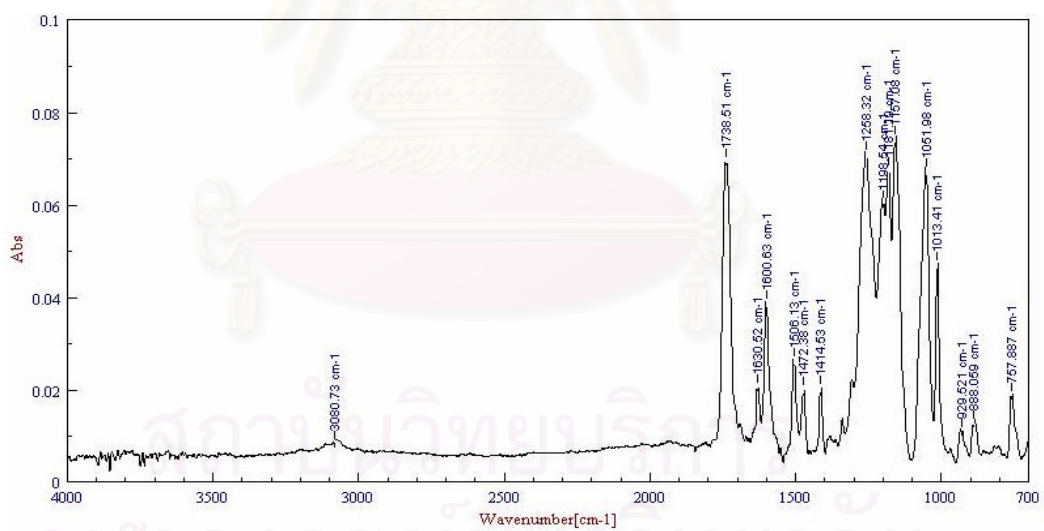


Figure 4.8 FTIR spectrum of liquid crystal polymer with 1 wt organoclay

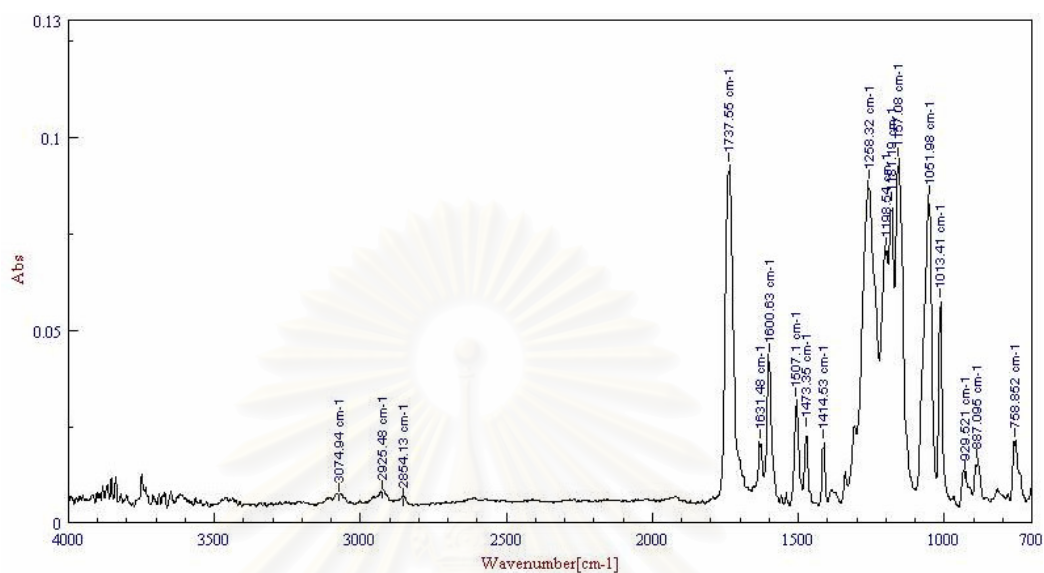


Figure 4.9 FTIR spectrum of liquid crystal polymer with 3 %wt organoclay

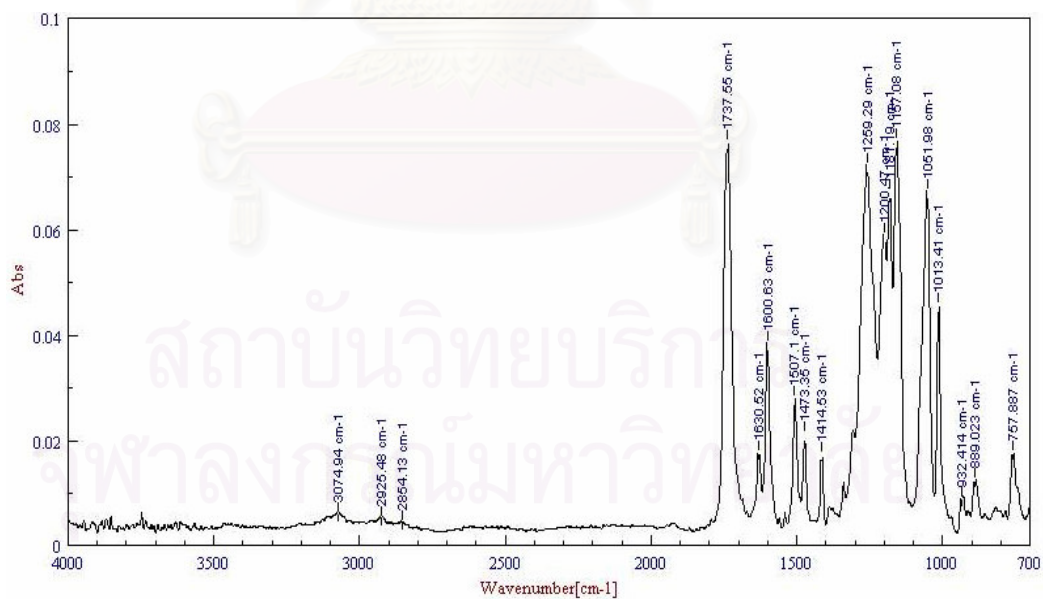


Figure 4.10 FTIR spectrum of liquid crystal polymer with 5 %wt organoclay

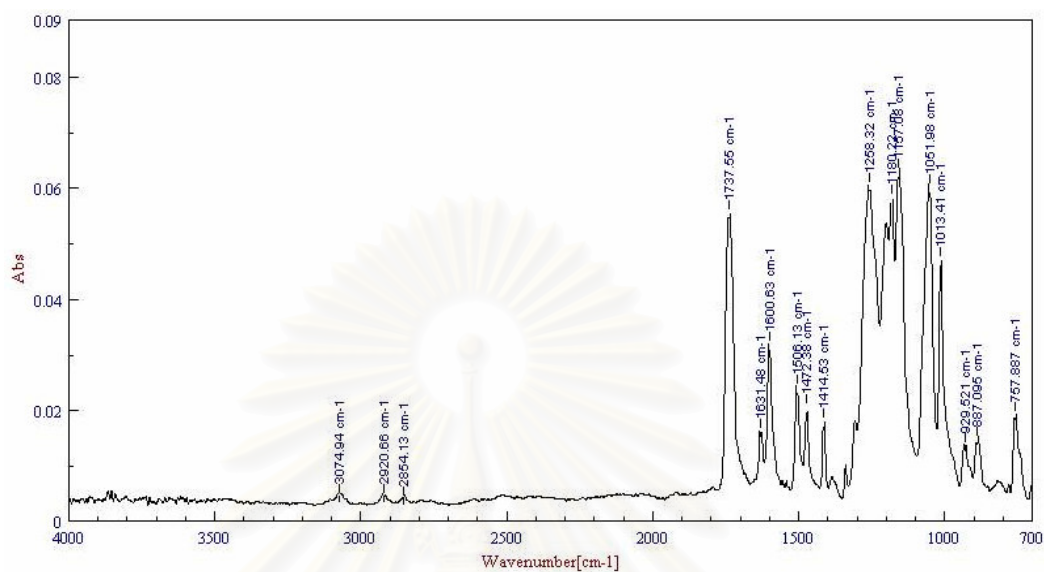


Figure 4.11 FTIR spectrum of liquid crystal polymer with 7 %wt organoclay

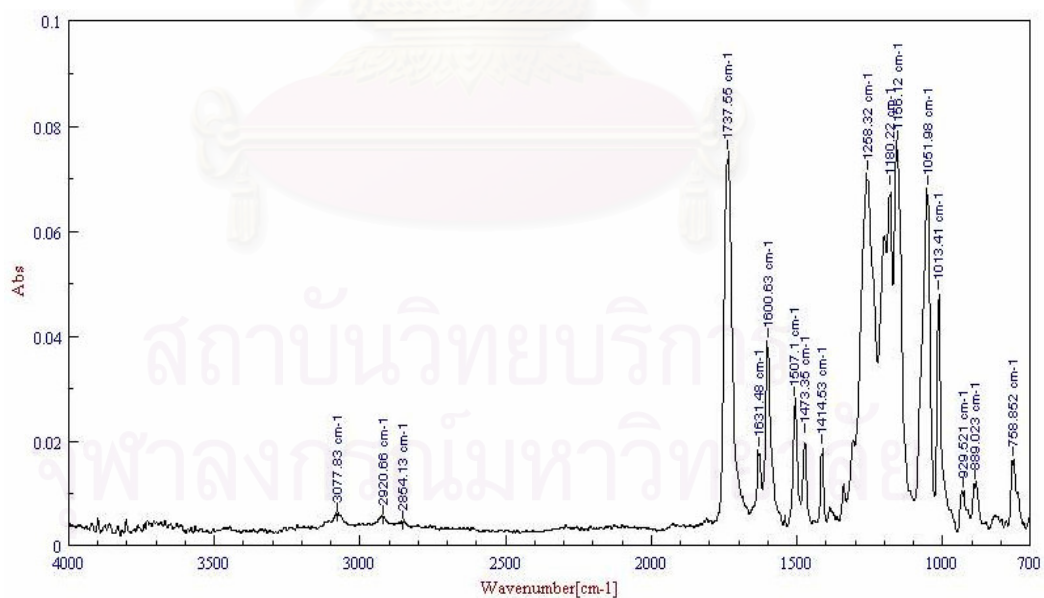


Figure 4.12 FTIR spectrum of liquid crystal polymer with 10 %wt organoclay

Table 4.5 Infrared band assignment of pure liquid crystal polymer and liquid crystal polymer/organoclay composite

Sample	Frequency cm^{-1}	Band assignment
Pure LCP	751, 888, 931	O-H out-of-plane bending of aromatic ring
LCP/organoclay 1 %wt	1031, 1051, 1157, 1181, 1201, 1258	C-O stretching
	1414, 1472, 1506, 1600, 1630	C=C stretching
	1738	C=O stretching
	3080	O-H stretching
LCP/organoclay 3, 5, 7, 10 %wt	751, 888, 931	O-H out-of-plane bending of aromatic ring
	1031, 1051, 1157, 1181, 1201, 1258	C-O stretching
	1414, 1472, 1506, 1600, 1630	C=C stretching
	1738	C=O stretching
	2854	CH_2 symmetric stretching
	2925	CH_2 asymmetric stretching
	3080	O-H stretching

4.2.2 Morphology of liquid crystal polymer/organoclay composite

The morphology of tensile fracture of pure liquid crystal polymer and liquid crystal polymer/organoclay composite with various organoclay contents in the direction transverse to flow are shown in Figure 4.13. It was observed that the molecular chains of liquid crystal polymer tend to follow the flow direction of the melt. The fibrilla morphology can be developed in the fabrics of liquid crystal

polymer consequently. Liquid crystal polymer process by injection moulding would give structural distribution since the process involves complex shear and extensional stress profile. The fibrilla liquid crystal polymer increased with the organoclay contents added. With increasing organoclay content, fibrous liquid crystal polymer was longer than unfilled polymer. The addition of organoclay fillers improved shear-induced fibrillation of the liquid crystal polymer in liquid crystal polymer/organoclay composite [37].



สถาบันวิทยบริการ
จุฬาลงกรณ์มหาวิทยาลัย

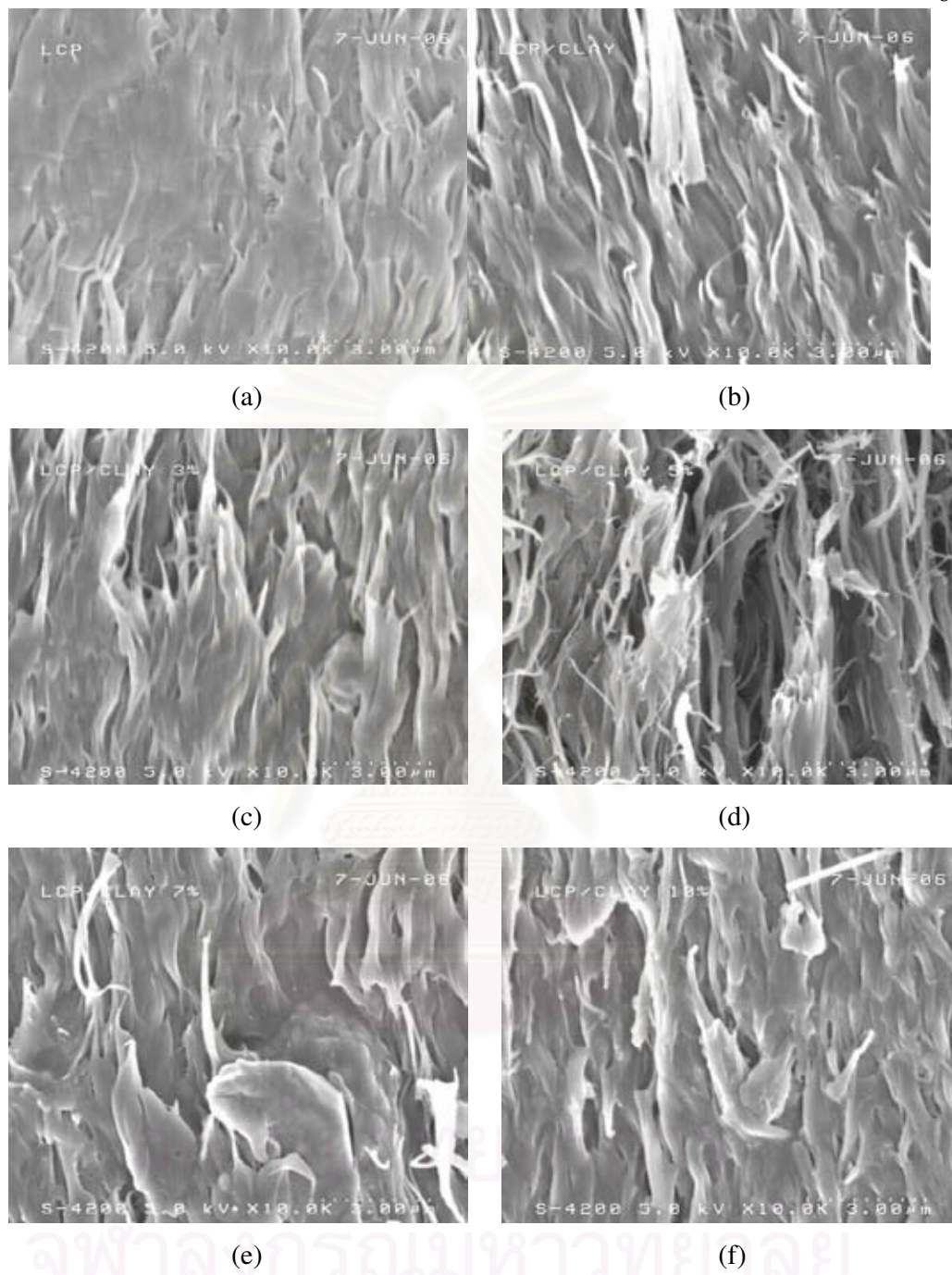


Figure 4.13 Morphology of liquid crystal polymer/organoclay composite at various organoclay contents;(a) Pure LCP, (b) LCP/organoclay 1 %wt, (c) LCP/organoclay 3 %wt, (d) LCP/organoclay 5 %wt, (e) LCP/organoclay 7 %wt, (f) LCP/organoclay 10 %wt

4.3 Mechanical properties

The mechanical properties of composites depend on many factors, including the aspect ratio of the filler, the degree of dispersion of the filler in the matrix resin and the adhesion at the filler matrix interface as shown in Tables 4.6-4.7.

Table 4.6 The tensile properties of LCP, LCP/organoclay composite and liquid crystal polymer with 30% glass fiber composite

Sample	Tensile strength (MPa)	Tensile modulus (MPa)
Pure LCP	130.31	5275.18
LCP/organoclay 1 %wt	136.81	6164.46
LCP/organoclay 3 %wt	146.15	6183.38
LCP/organoclay 5 %wt	150.51	6254.11
LCP/organoclay 7 %wt	151.93	6347.89
LCP/organoclay 10 %wt	153.33	6361.60
LCP/ 30% glass fiber	170.00	12000.00

Table 4.7 The flexural properties of LCP, LCP/organoclay composite and liquid crystal polymer with 30% glass fiber composite

Sample	Flexural strength (MPa)	Flexural modulus (MPa)
Pure LCP	158.78	8527.11
LCP/organoclay 1 %wt	153.33	8228.94
LCP/organoclay 3 %wt	152.23	8166.19
LCP/organoclay 5 %wt	152.40	8135.55
LCP/organoclay 7 %wt	146.34	7636.69
LCP/organoclay 10 %wt	145.68	7628.78
LCP/ 30% glass fiber	170.00	12000.00

With increasing clay loading, the tensile strength and tensile modulus of liquid crystal polymer/organoclay composite increase but liquid crystal polymer /organoclay composite have no potential to replace the liquid crystal polymer with 30% glass fiber as showed in Figure 4.14. This result was consistent with Gao F. [38] who reported clay/polymer nanocomposite cannot match fiber reinforced composites with high fiber volume fraction. While the flexural strength and flexural modulus decreases as shown in Figure 4.15. This result was also consistent with Lee et al. [37] who reported injection molding has a problem of producing anisotropic specimens which have low transverse flow direction properties.

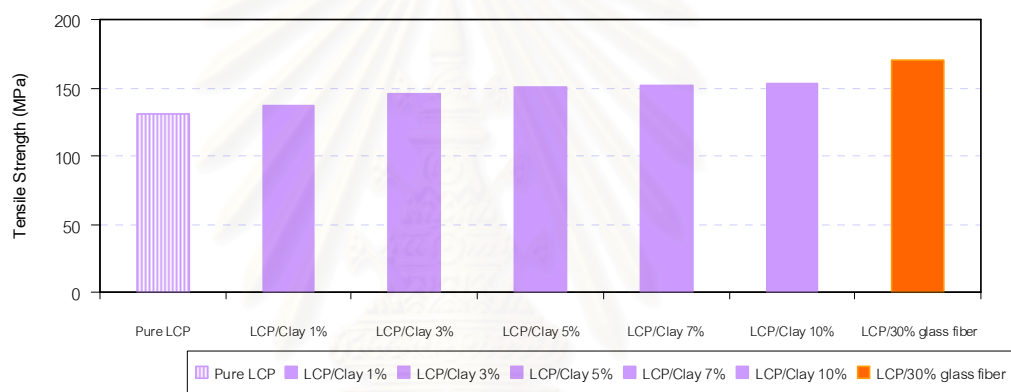


Figure 4.14 Tensile strength of liquid crystal polymer, liquid crystal polymer /organoclay composite and liquid crystal polymer with 30% glass fiber composite.

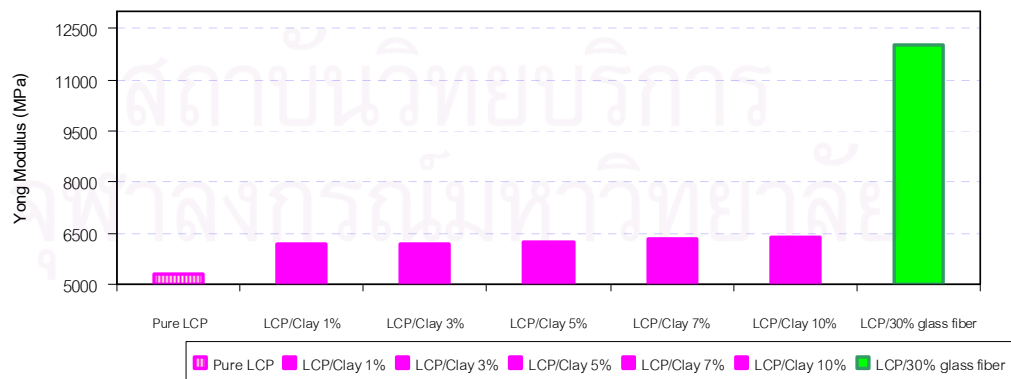


Figure 4.15 Young modulus of liquid crystal polymer, liquid crystal polymer /organoclay composite and liquid crystal polymer with 30% glass fiber composite.

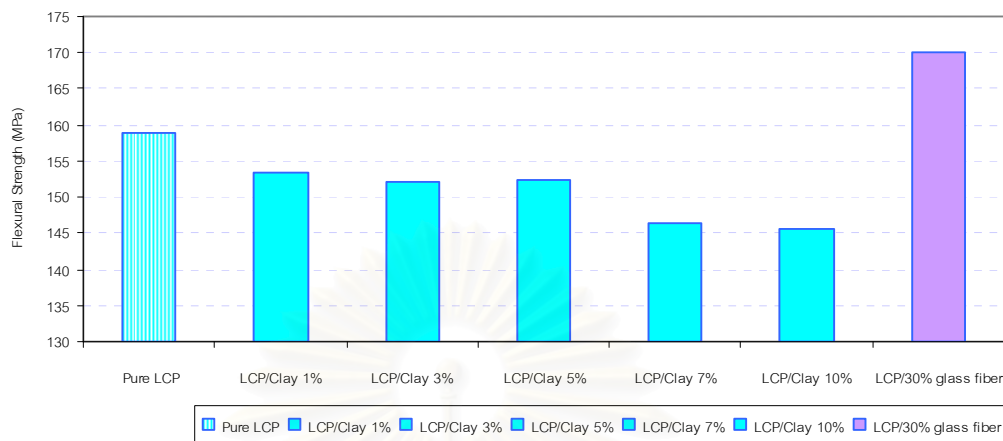


Figure 4.16 Flexural strength of liquid crystal polymer, liquid crystal polymer/organoclay composite and liquid crystal polymer with 30% glass fiber composite.

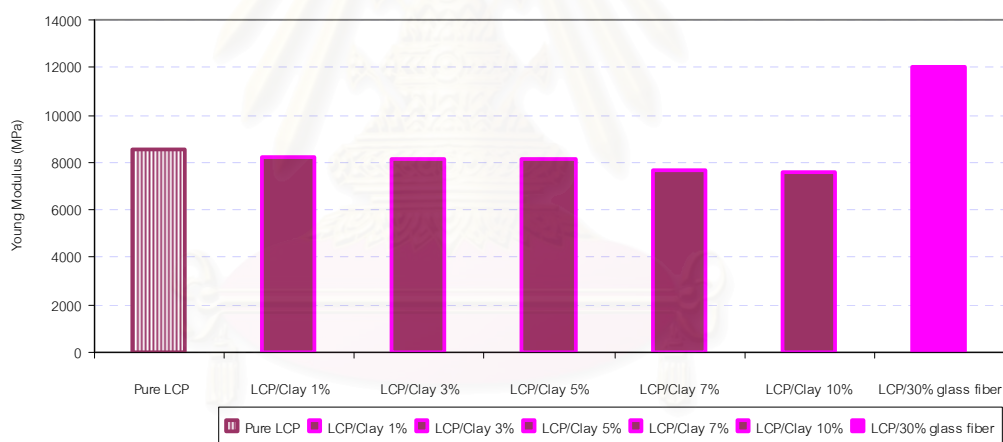


Figure 4.17 Flexural modulus of liquid crystal polymer, liquid crystal polymer/organoclay composite and liquid crystal polymer with 30% glass fiber composite.

4.4 Thermal property

The thermal stability of liquid crystal polymer and liquid crystal polymer/organoclay composite with difference organoclay contents in nitrogen and oxygen environment was investigated by TGA. TGA thermograms of liquid crystal

polymer and liquid crystal polymer/organoclay composite are shown in Figure 4.16. At the initial stage of the degradation (before 500 °C), due to the Hofmann elimination reaction and the clay catalysed degradation, the liquid crystal polymer/organoclay composite degrade faster than pure liquid crystal polymer and the % weight loss in temperature higher than 500 °C decreased with increase in the amount of organoclay. This was indicative that liquid crystal polymer/organoclay composites are more stable than pure liquid crystal polymer because % weight loss of liquid crystal polymer/organoclay composite less than % weight loss of pure liquid crystal polymer. The % weight loss data of liquid crystal polymer and liquid crystal polymer/organoclay composite are shown in Table 4.8.

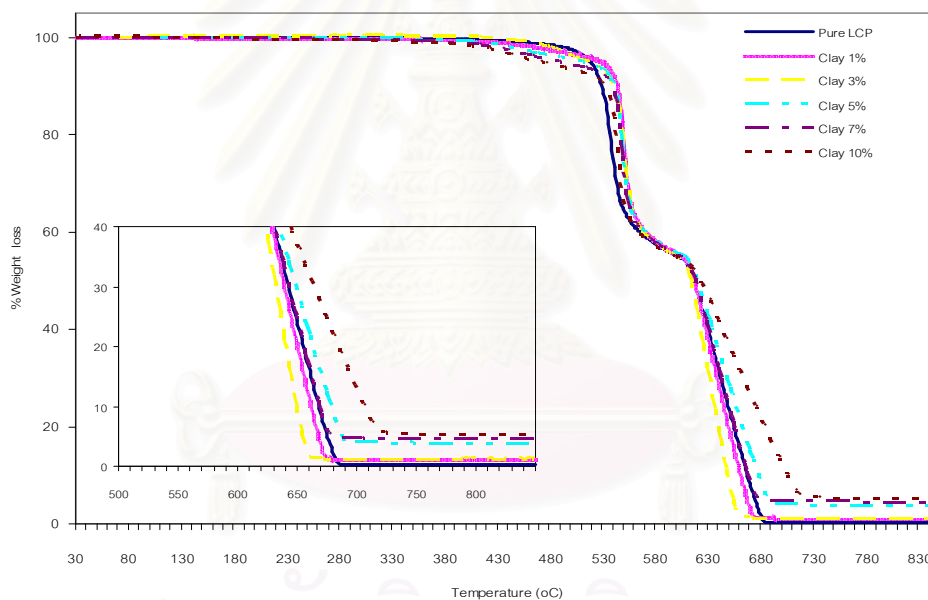
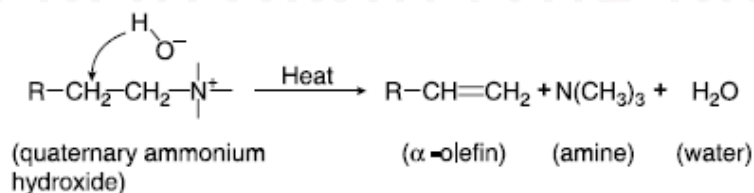


Figure 4.18 TGA thermogram of liquid crystal polymer and liquid crystal polymer/organoclay composite

Table 4.8 Weight loss percentages of liquid crystal polymer and liquid crystal polymer/organoclay composite

Sample	% Weight loss of liquid crystal polymer and liquid crystal polymer/organoclay at difference stages			
	500 °C	600 °C	700 °C	800 °C
Pure LCP	2.46	44.85	99.71	99.67
LCP/organoclay 1 %wt	3.33	44.55	98.97	99.05
LCP/organoclay 3 %wt	3.65	44.94	98.69	98.67
LCP/organoclay 5 %wt	4.49	44.12	95.89	96.08
LCP/organoclay 7 %wt	5.43	44.52	95.26	95.46
LCP/organoclay 10 %wt	6.47	45.10	87.38	94.70

TGA result showed the initial stage of degradation of liquid crystal polymer/organoclay composite which was lower than those of pure liquid crystal polymer due to the thermal decomposition of quaternary ammonium salt that was incorporated into clay surface modification. This suggested that the initial degradation of the organoclay follows a Hoffman elimination mechanism as shown in Scheme 4.1 for alkyl ammonium hydroxide) with the release of long chained α -olefins (C16–C18). All of them suggest the formation of alpha olefins, amines and other products resulting from the secondary reactions between the degradation products within the organoclay. Therefore, the introduction of quaternary ammonium salts in liquid crystal polymer/organoclay composite could reduce their initial stage of degradation [39].



Scheme 4.1 Hofmann elimination mechanism of quaternary ammonium salt

4.5 Flammability properties

Flame retardant of pure liquid crystal polymer and liquid crystal polymer/organoclay composite were evaluated by conventional testing methods using the vertical burning test (UL-94) and limiting oxygen index (LOI).

4.5.1 The vertical burning test (UL-94)

Burning test was investigated to determine UL-94 classification which provides only a qualitative classification of the samples. The test was carried out on 3 mm thick bars. UL-94 measures the ease which a polymer may be burned or extinguished. The results of the vertical burning test are shown in Table 4.9. The pure liquid crystal polymer and liquid crystal polymer/organoclay composite were extinguished and can be complied with V-0 requirements.

Table 4.9 UL-94 Classification of pure liquid crystal polymer and liquid crystal polymer/organoclay composite

Sample	UL-94 Classification
Pure LCP	V-0
LCP/organoclay (1 %wt)	V-0
LCP/organoclay (3 %wt)	V-0
LCP/organoclay (5 %wt)	V-0
LCP/organoclay (7 %wt)	V-0
LCP/organoclay (10 %wt)	V-0

4.5.2 Limiting Oxygen Index (LOI)

The limiting oxygen index was investigated to determine the flammability behavior of pure liquid crystal polymer and the liquid crystal polymer/organoclay composite. According to LOI procedure, the LOI value was taken as the minimum

percentages of oxygen required in a nitrogen-oxygen atmosphere, surrounding the sample, to maintain its combustion for at least 30 s after ignition. Hence, the LOI value of these samples can not be investigated because the samples immediately extinguished after remove the ignition flame even pure liquid crystal polymer.



สถาบันวิทยบริการ
จุฬาลงกรณ์มหาวิทยาลัย

CHAPTER V

CONCLUSION AND SUGGESTIONS FOR FUTURE WORK

5.1 Conclusion

Reactive intercalating agent was used to modify montmorillonite clay to obtain organophilic montmorillonite which predominate the interaction between liquid crystal polymer and organoclay. The chemical reaction with hydroxyl groups at the edge of clay layers and the interlayer ion-exchange were investigated by XRD, FTIR and elemental analysis. The increased interlayer spacing was confirmed that the surfactant was incorporated into organoclay layers. On the other hand, FTIR spectra and elemental analysis indicated that the surfactant molecules on montmorillonite were coordinated to exchangeable cations directly.

Liquid crystal polymer/organoclay composite were prepared by melt intercalation method. The XRD pattern indicated that the organoclay dispersed into liquid crystal polymer as shown by the increase in the interlayer spacing with organoclay at 3, 5, 7, 10 %wt content. This was confirmed that there was incorporation between the organoclay and polymer matrix as an intercalated type and FTIR spectra was ascribed to the delamination of organoclay layers into polymer matrix. While adding with low organoclay (1 %wt content), there was no peak of organoclay due to composite structure has been considered as exfoliated type and also FTIR spectra was not shown the interaction between organoclay and polymer matrix. Morphological structure was verified by SEM which showed that the fibrillation of liquid crystal polymer was improved with increasing organoclay content. The resulting composite exhibited considerable improvements in tensile property even incorporate with low organoclay (1%wt content) but its reduce flexural property. By adding organoclay, the thermal stability was improved but the surfactant decreased the thermal stability. The flammability properties were evaluated by UL-94 test, the

liquid crystal polymer/organoclay composite was achieved with V-0 requirements. Finally, the liquid crystal polymer/organoclay composite showed concurrent improvement in various material properties at very low filler content, together with the ease of preparation through simple processes such as injection moulding but low filler range up to 10%wt still can not be replaced the liquid crystal polymer reinforced with 30% glass fiber loading.

5.2 Suggestions for Future work

1. The mechanical and thermal properties of liquid crystal polymer/organoclay composite with other additives to optimize the mechanical and thermal properties should be studied.
2. The mechanical and thermal properties of liquid crystal polymer reinforced with 30% glass fiber loading blend with organoclay should be investigated.

REFERENCES

- [1.] Collings, P.J. Liquid Crystal, nature's delicate phase of matter. United States of America: Princeton University Press, 1990, 85-112.
- [2.] Elias, H.G. An Introduction to Polymer Science. Germany: VCH Weinheim, 1997, 165-176.
- [3.] Percec, V. Handbook of Liquid Crystal Research. New York: Oxford University Press, 1997, 259-346.
- [4.] Franek, J.; Jedlinski, Z.J. and Majnusz, J. Synthesis of polymeric liquid Crystals. In: Kricheldorf HR (ed) Handbook of Polymer Synthesis. Part B, Marcel Dekker, 1992, 1281-1351.
- [5.] Roggero, A. Application of liquid crystal polymers and thermotropic liquid crystal polymer blends. Pennsylvania: Technomic, Inc., 1993, 157-177.
- [6.] McChesney, C. Liquid crystal polymers (LCP). Engineering Plastic, Vol 2, In: Handbook of Engineering Materials. 1988, 179-182.
- [7.] MacDonald, W.A. Main chain liquid crystal polymers. Cambridge. Cambridge: The Royal Society of Chemistry, 1997, 428-453.
- [8.] Acieno, D.; and Nobile, M.R. Processing and properties of thermotropic liquid crystalline polymer. Pennsylvania: Technomic, Inc., 1993, 59-103.
- [9.] Moore, D. M.; Robert, C. and Reynolds, Jr. Identification of mixed-layered clay mineral: X-ray diffraction and the identification and analysis of clay minerals. 2nd ed. New York: Oxford University Press, 1997, 241-271.
- [10.] Weaver, C. and Pollard, L.D. The chemistry of clay minerals. New York: Elsevier Scientific, 1975, 115-213.
- [11.] Theng, B.K.G. The Chemistry of Clay-Organic Reactions. New York: Wiley, 1974, 261-291.
- [12.] Deer, W.A.; Howie, R.A. and Zussman. J. An Introduction to the rock-forming minerals. China: Addison Wesley Longmann, 1996, 418-442.
- [13.] Giannelis, E.P.; Krishnamoorti, R.; Manias, E. Polymer-Silica Nanocomposites: Model Systems for Confined Polymers and Polymer Brushes. Adv. Polym. Sci. 1999, 118, 108-147.

- [14.] Papke and Keith, G. Montmorillonite, Bentonite and Fuller's Earth Deposite in Nevada. Unites States of America: University of Nevada-Reno, 1970,76.
- [15.] Lagaly, G. Interaction of alkylamines with different types of layered compounds. Solid State Ionics 22(1986): 43-51.
- [16.] Hackett, E.; Manias, E. and Giannelis, E.P. Molecular dynamics simulations of organically modified layered silicates. J.Chem. Phys. 108(1998): 7410-7415.
- [17.] Yurudu, C.; Isci, S.; Unlu, C.; Atici, O.; Ece, O.I. and Gungor, N. Synthesis and characterization of HDA/NaMMT organoclay. Mater. Sci. Eng. 28(2005): 623-628.
- [18.] Ishida, H.; Campbell, S. and Blackwell, J. General approach to nanocomposite preparation. Chem. Mater. 12(2000): 1260-1267.
- [19.] Dubois, P. and Alexandre, M. Polymer-layered silicate nanocomposites: preparation, properties and use of a new class of materials. Mater. Sci. Eng. 28(2000): 1-63.
- [20.] Ray, S.S. and Okamoto, M. Polymer/layered silicate nanocomposites: a review from preparation to processing. Prog. Polym. Sci. 28(2003): 1539-1641.
- [21.] Vaia, R.A.; Jant. K.D.; Kramer, E.J. and Giannelis, E.P. Microstructural evaluation of melt-intercalated, polymer-organically modified layered silicate nanocomposites. Chem. Mater. 8(1996): 2628-2635.
- [22.] Israelachvili, J.N. Intermolecular and surface forces. New York: Academic Press, 1992, 450.
- [23.] Kojima, Y.; Usuki, A.; Kawasumi, M.; Okada, A.; Kurauchi, T. and Kamigaito O. One-pot synthesis of nylon-6/clay hybrid. J.Polym. Sci. 31(1993): 1755-1758.
- [24.] Liu, X. and Wu, Q. PP/Clay nanocomposites prepared by grafting melt intercalation. Polymer. 42(2001): 10013-10019.
- [25.] Sinha, R.; Yamada, K.; Okamoto, M. and Ueda, K. New polylactide/layered silicate nanocomposites. Polymer. 44(2003): 857-866.
- [26.] Zanetti, M.; Camina, G.; Thomann, R. and Mulhaupt, R. Synthesis and thermal behavior of layered silicate-EVA nanocomposites. Polymer. 42(2001): 4501-4507.

- [27.] Wang, S.; Hu, Y.; Zong, R.; Tang, Y.; Chen, Z. and Fan, W. Preparation and characterization of flame retardant ABS/Montmorillonite nanocomposite, Appl. Clay. Sci. 25(2004): 49-55.
- [28.] Kojima, Y.; Usuki, A.; Kawasumi, M.; Okada, A.; Fukushima, Y.; Karauchi, T. and Kamigaito, O. Mechanical properties of nylon-6-clay ybrid. J. Mater. Res. 6(1993): 1185-1189.
- [29.] Gilman, J.W. Flammability and thermal stability studies of polymer layered-silicate(clay) nanocomposites. Appl. Clay Sci. 15(1999): 31-49.
- [30.] Kawasumi, M.; Hasegawa, N.; Usaki, A. and Okada, A.; Liquid crystal/clay mineral composites. Appl. Clay Sci. 15(1999): 93-108.
- [31.] Zeng, Q.H.; Yu, A.B. and Lu, G.Q. Nanocomposites from polystyrene and layered clay minerals. Australia: Technology convergence in composites application, 2001, 549-553.
- [32.] Wang, Z.M.; Chung, T.C.; Gilman, J.W. and Manias, E. Melt-processable syndiotactic polystyrene/montmorillonite nanocomposites. J. Polym. Sci. 41(2003):3173-3187.
- [33.] Lee, M.W.; Hu, X.; Li, L.; Yue, C.Y.; Tam, K.C. and Cheong, L.Y. PP/LCP composites: effect of shear flow, extensional flow and nanofillers, Comp. Sci. 63(2003):1921-1929.
- [34.] Zhao, C.; Qin, H.; Gong, F.; Feng, H.; Zhang, S. and Yang, M. Mechanical, thermal and flammability properties of polyethylene/clay nanocomposites. Polym. Degrad. Stab. 87(2005):183-189.
- [35.] Ratna, D.; Diverkar, S.; Samui, A.B.; Chakraborty, B.C. and Banthia, A.K. Poly(ethylene oxide)/clay nanocomposite: Thermochemical properties and morphology. Polymer 47(2006): 4068-4074.
- [36.] Pavia, D.L.; Lampman, G.M. and Kriz, G.S. Introduction to Spectroscopy. United States of America: Western Washington University, 2001, 20-101.
- [37.] Lee, M.W.; Hu, X.; Li, L.; Yue, C.Y. and Tam, K.C. Effect of fillers on the structure and mechanical properties of LCP/PP/SiO₂ in-situ hybrid nanocomposites. Comp. Sci. 63(2003): 339-346.
- [38.] Gao, F. Clay/polymer composites: the story. Materials Today November(2004): 50-55.

- [39.] Shah, R.K. and Paul, D.R. Organoclay degradation in melt processed polyethylene nanocomposite. Polymer 47(2006):4075-4084.



สถาบันวิทยบริการ
จุฬาลงกรณ์มหาวิทยาลัย



APPENDICES

สถาบันวิทยบริการ
จุฬาลงกรณ์มหาวิทยาลัย

APPENDIX A : TWIN SCREW EXTRUDER

Twin screw extrusion is used extensively for mixing, compounding, or reacting polymeric materials. The flexibility of twin screw extrusion equipment allows this operation to be designed specifically for the formulation being processed. For example, the two screws may be corotating or counterrotating, intermeshing or nonintermeshing. In addition, the configurations of the screws themselves may be varied using forward conveying elements, reverse conveying elements, kneading blocks, and other designs in order to achieve particular mixing characteristics.

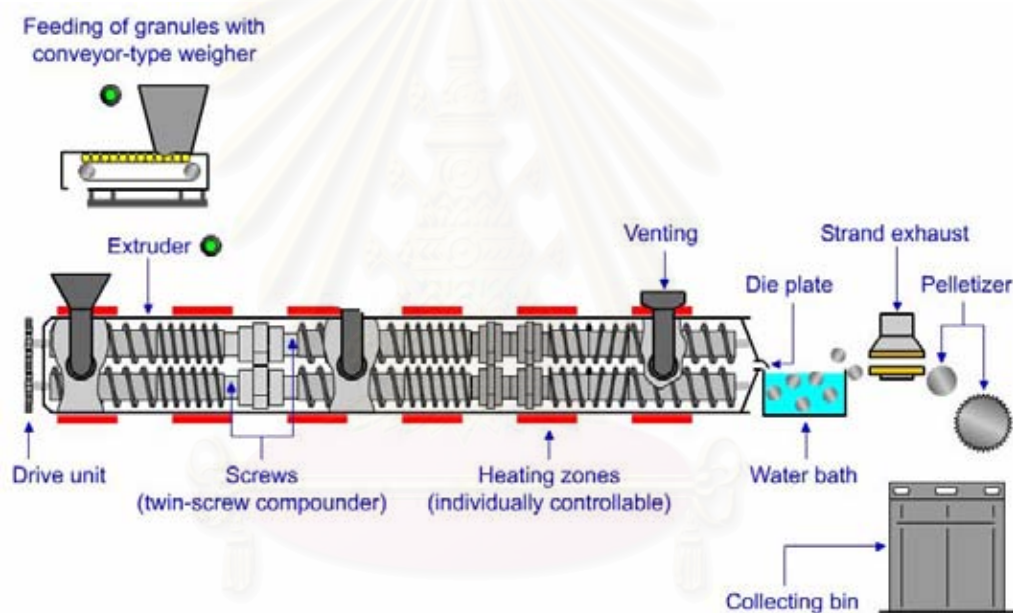


Figure A Twin screw extruder process schematic

APPENDIX B : INJECTION MOULDING

Injection molding is used extensively for the manufacture of polymeric items. A reciprocating/rotating screw both melts polymer pellets and provides the pressure required to quickly inject the melt into a cold mold. The polymer cools in the mold and the part is ejected.

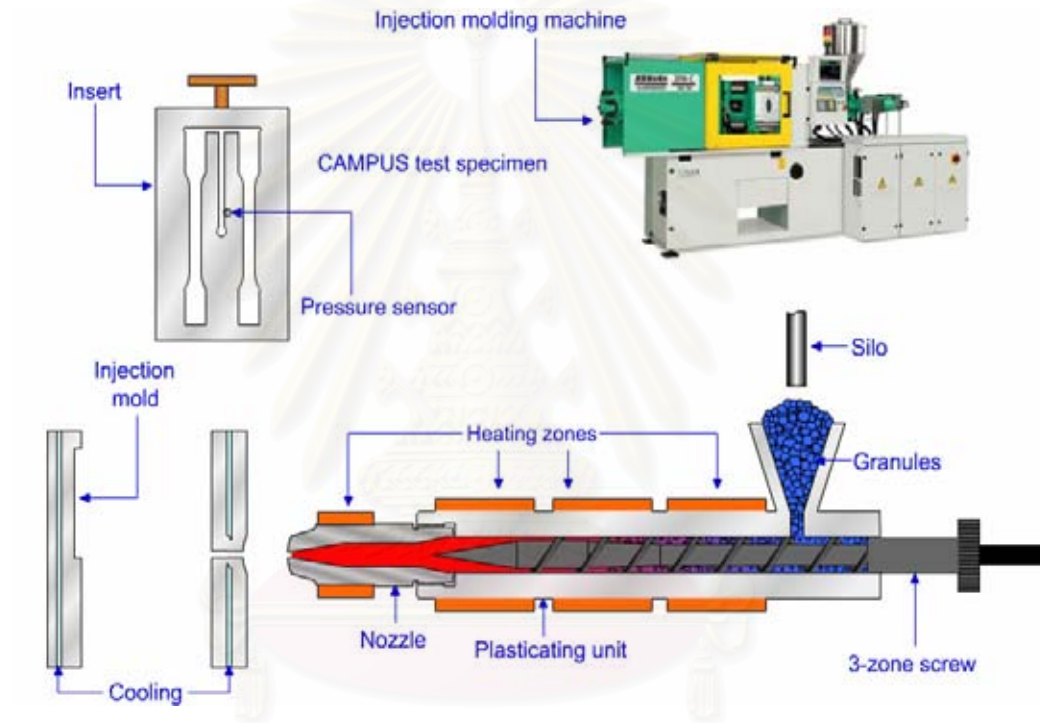


Figure B Injection process schematic

APPENDIX C : THE VERTICAL BURNING TEST

UL testing is a method of classifying a material's tendency to either extinguish or spread a flame once it has been ignited and although originally developed by UL. Vertical Burning Test (94V) is tested in the vertical orientation and the material burning at the lower end of the sample preheats the material in the upper areas of the specimen. A test flame is applied to the lower end of the test specimen and the material is classified according to the table below. UL-94V requires materials to be self-extinguishing to pass the test.

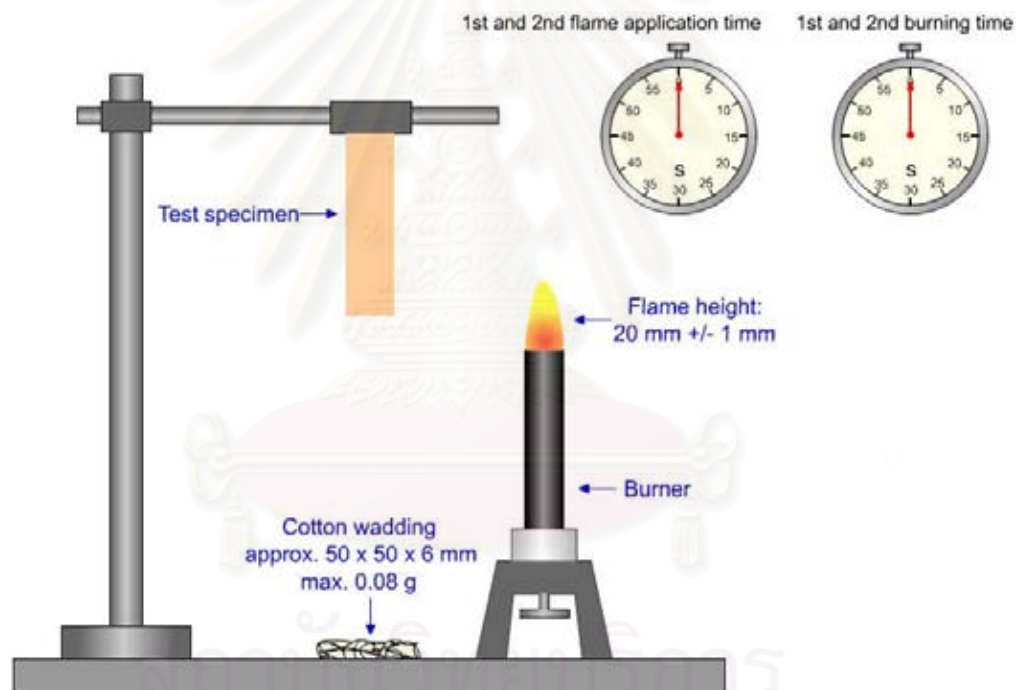


Figure C Vertical burning test for UL-94 Classification

Procedure

1. Clamp the specimen from the upper 6 mm of the specimen, with the longitudinal axis vertical, so that the lower end of the specimen is 300 +/- 10 mm above a horizontal layer of not more than 0.08 g of absorbent 100

percent cotton thinned to approximately 50x50 mm and a maximum thickness of 6 mm as show in Figure C.

2. The methane gas supply to the burner shall be arranged as in Figure C and adjusted to produce a gas flow rate of 105 ml/min with a back pressure than 10 mm of water.
3. Adjust the burner to produce a blue flame 20 +/- 1 mm high. The flame is obtained by adjusting the gas supply and air ports of the burner until a 20 +/- 1 mm yellow tipped blue flame is produced. Increase the air supply until the yellow tip just disappears. Measure the height of the flame again and readjust it if necessary.
4. Apply the flame centrally to the middle point of the bottom edge of the specimen so that the top of the burner is 10 +/- 1 mm below that point of the lower end of the specimen, and maintain it at that distance for 10 +/- 0.5 seconds, moving the burner as necessary in response to any changes in the length or position of the specimen. If the specimen drips molten or flaming material during the flame application, tilt the burner at an angle of up to 45 degree and withdraw it just sufficiently from beneath the specimen to prevent material from dropping into the base of the burner while maintaining the 10 +/- 1 mm spacing between the center of the top of the burner and the remaining portion of the specimen, ignoring any strings of molten material. After the application of the flame to the specimen for 10 +/- 0.5 seconds, immediately withdraw the burner at a rate of approximately 300 mm/sec, to a distance at least 150 mm away from the specimen and simultaneously commence measurement of the afterflame time t_1 in seconds. then record t_1 .
5. As soon as afterflaming of the specimen ceases, even if the burner has not been withdrawn to the full 150 mm distance from the specimen, immediately place the burner again under the specimen and maintain the burner at a distance o 10 +/- 1 mm from the remaining portion of the specimen for an additional 10 +/- 0.5 seconds, while moving the burner clear of dropping material as necessary. After this application of the flame to the specimen, immediately remove the burner at a rate of approximately 300 mm/sec to a distance of at least 150 mm from the

specimen and simultaneously commence measurement of the afterflame time, t_2 and the afterglow time, t_3 then record t_2 and t_3 .

Table C-1 Vertical burning test result of pure liquid crystal polymer

Criteria Conditions	V-0	Sample#1	Sample#2	Sample#3	Mean
Afterflame time after first flame application, t_1	$\leq 10s$	0.0	0.0	0.0	0.00
Afterflame time after second flame application, t_2	$\leq 10s$	0.0	0.5	0.0	0.16
Afterglow time after second flame Application, t_3	N/A	0.0	0.0	0.0	0.00
Afterflame plus afterglow time for each individual specimen after the second flame application ($t_2 + t_3$)	$\leq 30s$	0.0	0.5	0.0	0.16
Afterflame or afterglow of any Specimen up to the holding clamp	No	Pass	Pass	Pass	N/A
Cotton indicator ignited by flaming particles or drops	No	Pass	Pass	Pass	N/A

Table C-2 Vertical burning test result of Liquid crystal polymer/organoclay 1 %wt

Criteria Conditions	V-0	Sample#1	Sample#2	Sample#3	Mean
Afterflame time after first flame application, t_1	$\leq 10s$	0.0	0.0	0.0	0.00
Afterflame time after second flame application, t_2	$\leq 10s$	0.0	0.0	0.0	0.00
Afterglow time after second flame Application, t_3	N/A	0.0	0.0	0.0	0.00
Afterflame plus afterglow time for each individual specimen after the second flame application ($t_2 + t_3$)	$\leq 30s$	0.0	0.0	0.0	0.00
Afterflame or afterglow of any Specimen up to the holding clamp	No	Pass	Pass	Pass	N/A
Cotton indicator ignited by flaming particles or drops	No	Pass	Pass	Pass	N/A

สถาบันวิทยบริการ
จุฬาลงกรณ์มหาวิทยาลัย

Table C-3 Vertical burning test result of Liquid crystal polymer/organoclay 3 %wt

Criteria Conditions	V-0	Sample#1	Sample#2	Sample#3	Mean
Afterflame time after first flame application, t_1	$\leq 10s$	0.0	0.0	0.0	0.00
Afterflame time after second flame application, t_2	$\leq 10s$	0.0	0.0	0.5	0.16
Afterglow time after second flame Application, t_3	N/A	0.0	0.0	0.8	0.26
Afterflame plus afterglow time for each individual specimen after the second flame application ($t_2 + t_3$)	$\leq 30s$	0.0	0.0	1.3	0.43
Afterflame or afterglow of any Specimen up to the holding clamp	No	Pass	Pass	Pass	N/A
Cotton indicator ignited by flaming particles or drops	No	Pass	Pass	Pass	N/A

สถาบันวิทยบริการ
จุฬาลงกรณ์มหาวิทยาลัย

Table C-4 Vertical burning test result of Liquid crystal polymer/organoclay 5 %wt

Criteria Conditions	V-0	Sample#1	Sample#2	Sample#3	Mean
Afterflame time after first flame application, t_1	$\leq 10s$	1.1	0.0	0.0	0.36
Afterflame time after second flame application, t_2	$\leq 10s$	0.0	0.0	0.0	0.00
Afterglow time after second flame Application, t_3	N/A	0.0	0.0	0.0	0.00
Afterflame plus afterglow time for each individual specimen after the second flame application ($t_2 + t_3$)	$\leq 30s$	0.0	0.0	0.0	0.00
Afterflame or afterglow of any Specimen up to the holding clamp	No	Pass	Pass	Pass	N/A
Cotton indicator ignited by flaming particles or drops	No	Pass	Pass	Pass	N/A

สถาบันวิทยบริการ
จุฬาลงกรณ์มหาวิทยาลัย

Table C-5 Vertical burning test result of Liquid crystal polymer/organoclay 7 %wt

Criteria Conditions	V-0	Sample#1	Sample#2	Sample#3	Mean
Afterflame time after first flame application, t_1	$\leq 10s$	0.0	0.0	0.0	0.00
Afterflame time after second flame application, t_2	$\leq 10s$	0.8	1.0	1.5	1.10
Afterglow time after second flame Application, t_3	N/A	0.0	0.0	0.0	0.00
Afterflame plus afterglow time for each individual specimen after the second flame application ($t_2 + t_3$)	$\leq 30s$	0.8	1.0	1.5	1.10
Afterflame or afterglow of any Specimen up to the holding clamp	No	Pass	Pass	Pass	N/A
Cotton indicator ignited by flaming particles or drops	No	Pass	Pass	Pass	N/A

สถาบันวิทยบริการ
จุฬาลงกรณ์มหาวิทยาลัย

Table C-6 Vertical burning test result of Liquid crystal polymer/organoclay 10 %wt

Criteria Conditions	V-0	Sample#1	Sample#2	Sample#3	Mean
Afterflame time after first flame application, t_1	$\leq 10s$	0.6	0.5	0.0	0.36
Afterflame time after second flame application, t_2	$\leq 10s$	0.0	0.0	0.0	0.00
Afterglow time after second flame Application, t_3	N/A	0.0	0.0	0.0	0.00
Afterflame plus afterglow time for each individual specimen after the second flame application ($t_2 + t_3$)	$\leq 30s$	0.0	0.0	0.0	0.00
Afterflame or afterglow of any Specimen up to the holding clamp	No	Pass	Pass	Pass	N/A
Cotton indicator ignited by flaming particles or drops	No	Pass	Pass	Pass	N/A

สถาบันวิทยบริการ
จุฬาลงกรณ์มหาวิทยาลัย

APPENDIX D : MECHANICAL TESTING

Table D-1 Tensile Strength

Sample No.	Tensile Strength (MPa)					
	Pure LCP	LCP/organoclay 1 %wt	LCP/organoclay 3 %wt	LCP/organoclay 5 %wt	LCP/organoclay 7 %wt	LCP/organoclay 10 %wt
1	120.13	143.38	134.77	150.80	156.14	157.26
2	136.92	122.08	157.84	150.62	148.02	156.91
3	129.12	137.34	145.80	149.27	155.85	146.26
4	135.73	133.32	142.41	151.67	152.87	154.53
5	129.65	147.96	149.94	150.20	146.79	151.70
Mean	130.31	136.81	146.15	150.51	151.93	153.33
SD.	6.68	9.96	8.58	0.88	4.35	4.54

Table D-2 Tensile Modulus

Sample No.	Tensile Modulus (MPa)					
	Pure LCP	LCP/organoclay 1 %wt	LCP/organoclay 3 %wt	LCP/organoclay 5 %wt	LCP/organoclay 7 %wt	LCP/organoclay 10 %wt
1	5353.77	6182.41	6216.36	6405.61	6408.01	6501.80
2	5052.33	6210.65	6130.99	6201.85	6231.01	6512.50
3	5355.62	6392.87	5978.45	6113.10	6258.24	6264.99
4	5336.05	6214.67	6033.00	6105.94	6388.12	6135.79
5	5278.12	5821.70	6558.12	6444.07	6454.11	6392.96
Mean	5275.18	6164.46	6183.38	6254.11	6347.89	6361.61
SD.	128.47	208.95	228.51	160.94	97.74	161.04

Table D-3 Flexural Strength

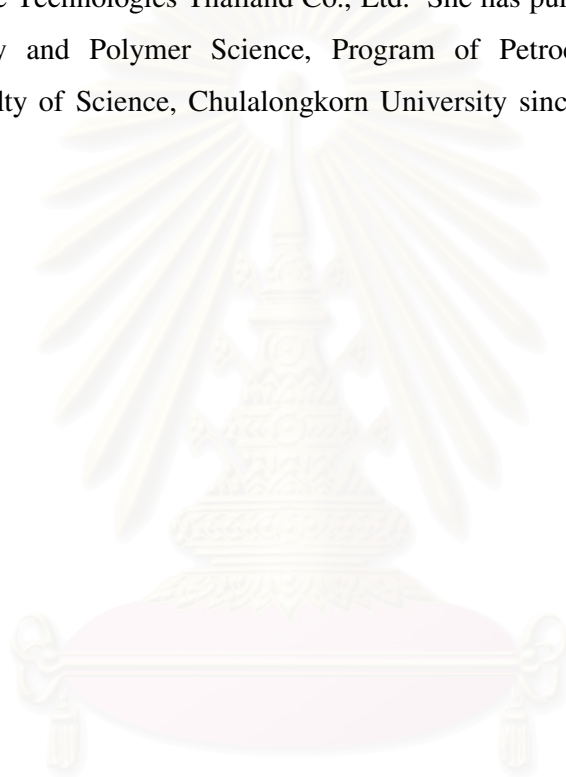
Sample No.	Flexural Strength (MPa)					
	Pure LCP	LCP/organoclay 1 %wt	LCP/organoclay 3 %wt	LCP/organoclay 5 %wt	LCP/organoclay 7 %wt	LCP/organoclay 10 %wt
1	159.36	156.81	150.71	151.25	147.78	141.46
2	162.45	153.23	153.03	152.76	145.17	147.58
3	159.50	152.03	151.62	148.90	144.73	149.85
4	155.97	155.92	150.33	154.27	149.90	143.69
5	156.62	148.69	155.45	154.84	144.11	145.81
Mean	158.78	153.33	152.23	152.40	146.34	145.68
SD.	2.59	3.24	2.08	2.41	2.43	3.27

Table D-4 Flexural Modulus

Sample No.	Flexural Modulus (MPa)					
	Pure LCP	LCP/organoclay 1 %wt	LCP/organoclay 3 %wt	LCP/organoclay 5 %wt	LCP/organoclay 7 %wt	LCP/organoclay 10 %wt
1	8298.05	8497.31	8114.71	7948.57	7648.73	7508.48
2	8584.00	8270.41	8138.40	8226.50	7486.53	7382.35
3	8602.28	8003.44	8093.79	7716.00	7847.64	8114.95
4	8645.21	8395.34	7956.38	8464.48	7847.64	7510.10
5	8506.02	7978.22	8527.69	8322.23	7544.11	7628.04
Mean	8527.11	8228.94	8166.19	8135.55	7636.69	7628.78
SD.	137.61	231.92	214.11	300.96	137.98	285.3

VITAE

Miss Busadee Homniam was born on December 30,1977, in Nakhon Sawan, Thailand. She received her Bachelor's degree in Materials Science, from the Faculty of Science, Chiang Mai University in 1999. She worked as an Engineer in Hitachi Global Storage Technologies Thailand Co., Ltd. She has pursued Master's Degree in Petrochemistry and Polymer Science, Program of Petrochemistry and Polymer Science, Faculty of Science, Chulalongkorn University since 2003 and finished her study in 2006.



สถาบันวิทยบริการ
จุฬาลงกรณ์มหาวิทยาลัย